

# Integrable aspects of the scaling $q$ -state Potts models I: bound states and bootstrap closure

Patrick Dorey<sup>1</sup>, Andrew Pocklington<sup>2</sup> and Roberto Tateo<sup>3</sup>

<sup>1,3</sup>*Dept. of Mathematical Sciences, University of Durham, Durham DH1 3LE, UK*

<sup>2</sup>*IFT/UNESP, Instituto de Fisica Teorica, 01405-900, Sao Paulo - SP, Brasil*

## Abstract

We discuss the  $q$ -state Potts models for  $q \leq 4$ , in the scaling regimes close to their critical or tricritical points. Starting from the kink S-matrix elements proposed by Chim and Zamolodchikov, the bootstrap is closed for the scaling regions of all critical points, and for the tricritical points when  $4 > q \geq 2$ . We also note a curious appearance of the extended last line of Freudenthal's magic square in connection with the Potts models.

---

<sup>1</sup>e-mail: p.e.dorey@durham.ac.uk

<sup>3</sup>e-mail: roberto.tateo@durham.ac.uk

# 1 Introduction

The  $q$ -state Potts models directly generalise the most well-known of all two-dimensional integrable models, the Ising model. They have been much studied, both in their own right as interesting statistical-mechanical systems, and because of their relations with other models – the limit  $q \rightarrow 1$ , for example, describes bond percolation. However, they are by no means completely understood.

In this paper and its sequel we shall discuss the treatment of these models in the framework of continuum field theory. Such techniques are expected to be applicable in scaling regimes near to critical points, though for the  $q$ -state Potts models some elements of the treatment will be rather formal, reflecting the nonlocal manner in which the models are initially defined on the lattice. In this paper we focus on the description of the models in terms of the on-shell data provided by an exact S-matrix. A number of years ago, Chim and Zamolodchikov proposed a set of amplitudes for the scattering of elementary kink-like excitations in the low-temperature phase of the model [1]. (A different treatment had previously been suggested by Smirnov [2], based on quantum-group reductions of the Izergin-Korepin S-matrix. In this article we shall work from the Chim-Zamolodchikov formulation, as it more closely reflects the continuous nature of the Fortuin-Kasteleyn [3] definition of the theory on a lattice, but we note that the relationship between the two approaches has recently been clarified, in [4].) The fundamental S-matrix elements form only part of the on-shell description of the model, and in order to complete the picture it is necessary to find out if any further asymptotic states are present. In the exact S-matrix framework this is commonly achieved by an analysis of the pole structure of all S-matrix elements, a process which is known as closure of the bootstrap. The case of the  $q$ -state Potts models turns out to involve a number of subtleties, which we attempt to highlight and resolve in this paper. Since we have not been entirely successful in this enterprise, we also include some details of the problems that we encountered. They only arose when continuing the S-matrices far into the regime of tricritical models, but they may nonetheless be important signals of new behaviour in the bootstrap programme.

In §2, we review Chim and Zamolodchikov's proposal and its background, stressing some of the non-standard features that the models exhibit. Then in §3 we close the bootstrap for the scaling regions of all critical models, finding that we need to invoke the Coleman-Thun mechanism in a novel way in order to explain the full pole structure of all S-matrix elements. A continuation of Chim and Zamolodchikov's S-matrix is expected to describe the scaling regions of the tricritical models, and this is discussed in §4. Finally, §5 contains our conclusions and some more detailed tables are collected in four appendices.

In a companion paper [5], these models will be discussed from a complementary point of view, using finite-size effects.

## 2 Review

### 2.1 The models on the lattice and their continuum limits

The standard definition of the lattice  $q$ -state Potts model is through the Hamiltonian

$$\mathcal{H} = -J \sum_{\langle x,y \rangle} \delta_{\sigma(x),\sigma(y)} \quad (2.1)$$

where  $J$  is a coupling strength and the spin  $\sigma(x)$  associated with the lattice site  $x$  may take any of  $q$  distinct values. The summation is over all nearest-neighbour pairs of sites  $\langle x,y \rangle$ . In terms of  $\mathcal{H}$ , the partition function at temperature  $T$  is given by

$$\mathcal{Z} = \sum_{\{\sigma\}} e^{-\frac{1}{kT} \mathcal{H}}. \quad (2.2)$$

Notice that  $\mathcal{H}$  is invariant under the group  $S_q$  of permutations of the  $q$  possible values of  $\sigma$ .

This definition only applies for integer values of  $q$ , but a reformulation due to Fortuin and Kasteleyn [3] allows the constraint to be lifted. Expanding (2.2) as

$$\mathcal{Z} = \sum_{\{\sigma\}} \prod_{\langle x,y \rangle} \left( 1 + (e^{\frac{J}{kT}} - 1) \delta_{\sigma(x),\sigma(y)} \right) \quad (2.3)$$

they observed that it could be written in the form

$$\mathcal{Z} = \sum_{\mathcal{G}} K^\nu q^C \quad (2.4)$$

where  $K = e^{\frac{J}{kT}} - 1$ , and the sum is over all graphs  $\mathcal{G}$  on the lattice, with  $\nu$  the number of bonds in  $\mathcal{G}$  and  $C$  the number of connected components (sets of sites joined by bonds). When the model is defined in this way,  $q$  is no longer restricted to integer values, and can be taken as a continuous parameter. However, at general values of  $q$ ,  $\mathcal{Z}$  cannot be written in terms of a local Hamiltonian, and the precise meaning of its ‘ $S_q$ ’ symmetry is not clear. Nevertheless, the partition function is certainly well-defined, and we shall see later that many other features which might be thought special to locally-defined theories also make sense.

The model undergoes a phase transition at  $K = K_c = \sqrt{q}$ , which is second-order for  $q \leq 4$ . At these values of  $q$  a continuum limit can be taken, and if the limit is taken exactly at the critical point, the resulting field theory is conformal. Parametrising  $q$  as

$$\sqrt{q} = 2 \sin \gamma = 2 \cos \left( \frac{\pi}{\xi+1} \right) \quad (2.5)$$

with  $0 \leq \gamma \leq \pi/2$  and  $\xi = (\pi+2\gamma)/(\pi-2\gamma)$ , its central charge is [6]

$$c(q) = 1 - \frac{6}{\xi(\xi+1)}. \quad (2.6)$$

A generalisation of the basic Potts model allows for the existence of vacancies [7]. In addition to the critical points just discussed, these models have tricritical points, with the critical and tricritical points coinciding at  $q = 4$ . The exponents for the tricritical points can be obtained from those of the critical points by continuing  $\gamma$  into the range  $\pi/2 \leq \gamma \leq \pi$  [7] (see also [8, 9]). This shifts  $\xi$  into the range  $-\infty < \xi < -3$ .

If  $\xi$  is rational, the value of  $c(q)$  coincides with the central charge  $c = 1 - 6(p' - p)^2 / pp'$  of a minimal model  $\mathcal{M}_{pp'}$ ,  $p' > p$ . More precisely, the relationship is

$$\xi = \frac{p}{p' - p} \tag{2.7}$$

on the critical branch, and

$$\xi = \frac{p'}{p - p'} \tag{2.8}$$

on the tricritical branch. This coincidence does *not* mean that the conformal field theories of the Potts models at rational  $\xi$  are minimal models – in particular, the relevant partition functions only agree when  $q$  is an integer [10] – but it does mean that connections with minimal models are to be expected at these points.

Other aspects of the critical and tricritical models, and of their relationships with conformal field theories, are reviewed in [5]. However in this paper we are more concerned with the massive field theories which arise if a continuum limit is taken with the temperature (and any other parameters) tending to a critical value with the correlation length held finite in physical units. In many interesting cases (including the ones currently under discussion [2, 1]) these field theories turn out to be integrable [11], allowing them to be understood in considerable detail. In turn, this allows the scaling regions of the original lattice models near to their second-order transitions to be explored; it is also relevant to the computation of certain universal characteristics of the transitions themselves [12].

In practice, the field theories are usually found directly in the continuum, either by a consideration of the symmetries that they should inherit from the lattice, or by starting from the continuum conformal field theories, and then adding to their actions suitable continuum operators to describe the departure from criticality – the basic idea of perturbed conformal field theory, as put forward by Zamolodchikov [11]. For shifts in temperature, the operator to add is the local energy density, which corresponds to  $\phi_{21}$  for the critical Potts models [6], and  $\phi_{12}$  for the tricritical models [13]. We shall refer to the massive theories as the scaling Potts models. Strictly speaking, they are not perturbations of minimal conformal field theories, except at integer values of  $q$ . However, in situations where the infinite-volume ground states of the  $q$ -state Potts and minimal models coincide, we expect the two to agree on issues such as mass spectrum and (diagonal) S-matrix elements. We shall say a little more about this issue in later sections and in [5], but since it is not directly relevant to our current discussion of the Potts S-matrices, we leave it to one side for now.

Irrespective of whether the unperturbed  $c < 1$  theories are minimal models, Zamolodchikov's counting argument [11] shows that generic  $\phi_{21}$  or  $\phi_{12}$  perturbations preserve

conserved charges with spins  $s = 1, 5, 7$  and  $11$ . By an argument due to Parke [14], the existence of these charges is enough to ensure that, as quantum field theories defined in Minkowski space, the models must have factorisable S-matrices, allowing the full multi-particle S-matrix to be given in terms of the set of two-particle scattering amplitudes\*. The main result of Chim and Zamolodchikov [1] was a conjecture for these amplitudes for certain fundamental, kink-like excitations. To finish the story, amplitudes for the scattering of all possible bound states of these kinks must be found, and this is the main goal of the present paper. In the remainder of this section, we shall review the assumptions that went into Chim and Zamolodchikov's initial proposal.

## 2.2 The fundamental S-matrix elements

To begin, we discuss the scaling regions of the *critical* models. The scattering theory is most easily treated by working in the low-temperature, ordered phase, in which one would expect to find  $q$  degenerate vacua. It is then natural to postulate the existence of a set of particles, or kinks,  $K_{ab}(\theta)$  ( $a, b = 1 \dots q$ ;  $a \neq b$ ), domain walls which interpolate between different vacua. The fact that  $q$  is not necessarily an integer may appear worrisome, but following [1] we can decide to treat  $q$  formally, motivated at least in part by the fact that this can be given a precise sense on the lattice through the Fortuin-Kasteleyn trick reviewed above. The energy-momentum of  $K_{ab}(\theta)$  is parameterized by the rapidity  $\theta$ ,  $p^\mu = (m \cosh \theta, m \sinh \theta)$ , and asymptotic  $n$ -particle states interpolating between vacua  $a_0$  and  $a_n$  correspond to the products

$$K_{a_0 a_1}(\theta_1) K_{a_1 a_2}(\theta_2) \dots K_{a_{n-1} a_n}(\theta_n) \quad (a_i \neq a_{i+1}) . \quad (2.9)$$

Scattering of these kinks is completely described by the two-particle amplitudes  $\mathcal{S}_{ac}^{bd}(\theta)$ :

$$K_{ab}(\theta_1) K_{bc}(\theta_2) = \sum_{d \neq a, c} \mathcal{S}_{ac}^{bd}(\theta) K_{ad}(\theta_2) K_{dc}(\theta_1) , \quad \theta = \theta_1 - \theta_2 . \quad (2.10)$$

Due to the  $S_q$  symmetry of the model, there are only four independent two-particle amplitudes  $\mathcal{S}^n(\theta)$  ( $n = 0 \dots 3$ ). These are represented in figure 1.

The S-matrix must be unitary, crossing symmetric, and satisfy the Yang-Baxter equations. Chim and Zamolodchikov found that the latter implies

$$\mathcal{S}^0(\theta) = \sin(\gamma) \sin(i\lambda\theta) \sin(3\gamma + i\lambda\theta) R(\theta) \quad (2.11)$$

$$\mathcal{S}^1(\theta) = \sin(2\gamma) \sin(\gamma + i\lambda\theta) \sin(3\gamma + i\lambda\theta) R(\theta) \quad (2.12)$$

$$\mathcal{S}^2(\theta) = \sin(2\gamma) \sin(i\lambda\theta) \sin(2\gamma + i\lambda\theta) R(\theta) \quad (2.13)$$

$$\mathcal{S}^3(\theta) = \sin(3\gamma) \sin(\gamma + i\lambda\theta) \sin(2\gamma + i\lambda\theta) R(\theta) \quad (2.14)$$

where  $\gamma$  is defined by  $2 \sin \gamma = \sqrt{q}$  as in (2.5) above, and  $\lambda$  is an as-yet undetermined parameter. Crossing symmetry requires that  $\mathcal{S}^0$  and  $\mathcal{S}^3$  be unchanged under  $\theta \rightarrow i\pi - \theta$

---

\*In all probability the models actually have conserved charges at all integer spins not multiples of 2 or 3, but just two with spins  $> 1$  are enough for Parke's argument to go through.

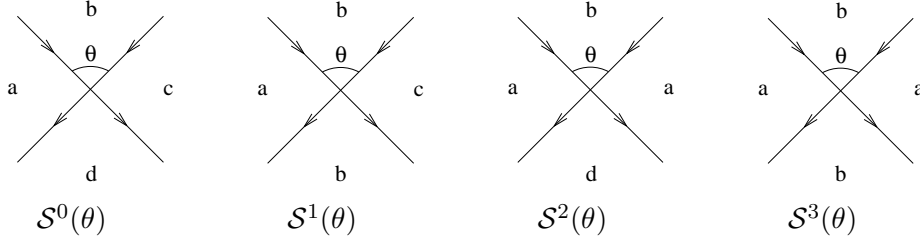


Figure 1: The four independent two-particle amplitudes

while  $\mathcal{S}^1$  and  $\mathcal{S}^2$  swap over, which implies  $\pi\lambda = 3\gamma \pmod{\pi}$  and  $R(i\pi - \theta) = R(\theta)$ . Unitarity then boils down to the condition

$$R(\theta)R(-\theta) = [\sin^2(\gamma) \sin(2\gamma + i\lambda\theta) \sin(2\gamma - i\lambda\theta) \sin(3\gamma + i\lambda\theta) \sin(3\gamma - i\lambda\theta)]^{-1} \quad (2.15)$$

Together with crossing, this fixes the S-matrix as a function of  $\gamma$  and  $\lambda$  up to a so-called CDD factor, a  $2\pi i$ -periodic function  $f$  satisfying  $f(\theta)f(-\theta) = 1$ ,  $f(i\pi - \theta) = f(\theta)$ . To resolve the remaining ambiguities, some further physical input is required, and this comes from an initial consideration of the pole structure.

In general, it should be possible to explain all S-matrix poles in the physical strip

$$0 \leq \Im m \theta \leq \pi \quad (2.16)$$

in terms of the bound-state structure of the model (though, as we shall see, the mechanism can in some cases be quite involved). Conversely, the fundamental S-matrix elements should certainly exhibit poles reflecting the possibility to form an elementary kink as a bound state of two other such kinks. Taking energy-momentum conservation and vacuum structure into account, direct-channel poles should appear in  $\mathcal{S}^0(\theta)$  and  $\mathcal{S}^1(\theta)$  at  $\theta = \frac{2\pi i}{3}$ , and cross-channel poles in  $\mathcal{S}^0(\theta)$  and  $\mathcal{S}^2(\theta)$  at  $\theta = \frac{\pi i}{3}$ . These are illustrated in figures 2 and 3.

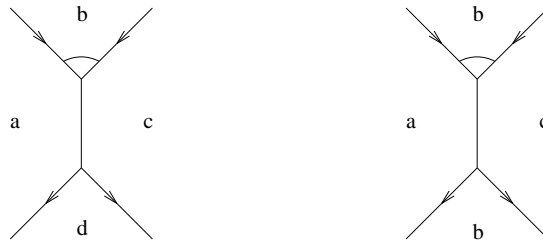


Figure 2: Direct channel  $KK \rightarrow K$  bound states in  $\mathcal{S}^0$  and  $\mathcal{S}^1$



Figure 3: Cross channel  $KK \rightarrow K$  bound states in  $\mathcal{S}^0$  and  $\mathcal{S}^2$

A comparison with (2.11) – (2.13) shows that the common factor  $R(\theta)$  must therefore have poles at  $\frac{\pi i}{3}$  and  $\frac{2\pi i}{3}$ . On the other hand, the pole at  $\frac{2\pi i}{3}$  should be absent from  $\mathcal{S}^2$  and  $\mathcal{S}^3$ , and the pole at  $\frac{\pi i}{3}$  absent from  $\mathcal{S}^1$  and  $\mathcal{S}^3$ . This can only be achieved by cancellations against zeroes from the sine prefactors in (2.12) – (2.14), which strengthens the previous condition on  $\lambda$  to  $\pi\lambda = 3\gamma \pmod{3\pi}$ .

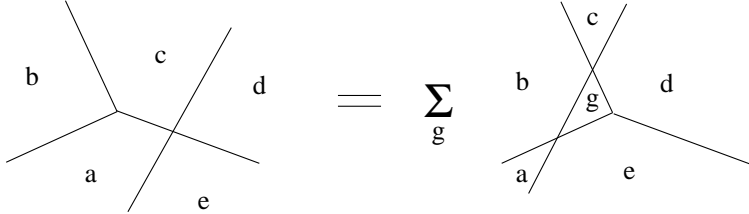


Figure 4:  $KK \rightarrow K$  bootstrap

The three-kink coupling leads to a set of bootstrap equations, depicted in figure 4. In contrast to the Yang-Baxter equations, these constraints are felt by the CDD factor. Combining these conditions with a prior knowledge of the solutions for  $q = 2$  and  $3$  led Chim and Zamolodchikov to the simplest choice  $\pi\lambda = 3\gamma$ , and a minimal solution for the S-matrix elements which, for the discussions to come, it will be most convenient to rewrite in the following form:

$$\mathcal{S}^0(\theta) = \frac{\sinh(\lambda\theta)}{\sinh(\lambda(\theta - \frac{2\pi i}{3}))} S(\theta), \quad (2.17)$$

$$\mathcal{S}^1(\theta) = \frac{\sin(\frac{2\pi\lambda}{3}) \sinh(\lambda(\theta - \frac{\pi i}{3}))}{\sin(\frac{\pi\lambda}{3}) \sinh(\lambda(\theta - \frac{2\pi i}{3}))} S(\theta), \quad (2.18)$$

$$\mathcal{S}^2(\theta) = \frac{\sin(\frac{2\pi\lambda}{3}) \sinh(\lambda\theta)}{\sin(\frac{\pi\lambda}{3}) \sinh(\lambda(\theta - i\pi))} S(\theta), \quad (2.19)$$

$$\mathcal{S}^3(\theta) = \frac{\sin(\lambda\pi) \sinh(\lambda(\theta - \frac{\pi i}{3}))}{\sin(\frac{\pi\lambda}{3}) \sinh(\lambda(\theta - i\pi))} S(\theta). \quad (2.20)$$

The overall scalar factor  $S(\theta)$  is

$$S(\theta) = \frac{\sinh(\lambda(\theta + \frac{\pi i}{3}))}{\sinh(\lambda(\theta - \frac{\pi i}{3}))} e^{\mathcal{A}(\theta)} \quad (2.21)$$

with  $e^{\mathcal{A}(\theta)}$  defined in terms of the blocks

$$\mu(a) = \frac{\Gamma(a - \frac{\lambda}{i\pi}\theta) \Gamma(a + \lambda + \frac{\lambda}{i\pi}\theta)}{\Gamma(a + \frac{\lambda}{i\pi}\theta) \Gamma(a + \lambda - \frac{\lambda}{i\pi}\theta)} = \exp \left[ 2 \int_0^\infty \frac{dx}{x} \sinh(\frac{\lambda}{i\pi}\theta x) e^{-ax} \frac{(1 - e^{-\lambda x})}{(1 - e^{-x})} \right] \quad (2.22)$$

as

$$e^{\mathcal{A}(\theta)} = \prod_{k=0}^{\infty} \frac{\mu(1 + 2k\lambda)}{\mu((2k+1)\lambda)} \frac{\mu(1 + (2k - \frac{1}{3})\lambda)}{\mu((2k + \frac{4}{3})\lambda)}. \quad (2.23)$$

From the second equality in (2.22) and the formula

$$\frac{\sinh(\lambda(\theta + i\pi\alpha))}{\sinh(\lambda(\theta - i\pi\alpha))} = \exp \left[ -2 \int_0^\infty \frac{dk}{k} \sinh(ik\theta) \frac{\sinh(\frac{\pi k}{2}(\frac{1}{\lambda} - 2\alpha))}{\sinh(\frac{\pi k}{2\lambda})} \right] \quad (2.24)$$

it is a simple matter to recover integral representations equivalent to those given in [12]:

$$\mathcal{A}(\theta) = -2 \int_0^\infty \frac{dk}{k} \sinh(ik\theta) \frac{\cosh(\frac{\pi k}{6}) \sinh(\frac{\pi k}{2}(\frac{4}{3} - \frac{1}{\lambda}))}{\cosh(\frac{\pi k}{2}) \sinh(\frac{\pi k}{2\lambda})}; \quad (2.25)$$

$$\log S(\theta) = -2 \int_0^\infty \frac{dk}{k} \sinh(ik\theta) \frac{\cosh(\frac{\pi k}{2}(\frac{1}{3} - \frac{1}{\lambda})) \sinh(\frac{\pi k}{3})}{\cosh(\frac{\pi k}{2}) \sinh(\frac{\pi k}{2\lambda})}. \quad (2.26)$$

In addition,  $e^{\mathcal{A}(\theta)}$  and  $S(\theta)$  satisfy

$$e^{\mathcal{A}(-\theta)} = e^{-\mathcal{A}(\theta)} \quad , \quad e^{\mathcal{A}(i\pi - \theta)} = \frac{\sinh(\lambda\theta)}{\sinh(\lambda(\theta - i\pi))} \frac{\sinh(\lambda(\theta + \frac{\pi i}{3}))}{\sinh(\lambda(\theta - \frac{4\pi i}{3}))} e^{\mathcal{A}(\theta)}; \quad (2.27)$$

$$S(-\theta) = 1/S(\theta) \quad , \quad S(i\pi - \theta) = \frac{\sinh(\lambda\theta)}{\sinh(\lambda(\theta - i\pi))} \frac{\sinh(\lambda(\theta - \frac{\pi i}{3}))}{\sinh(\lambda(\theta - \frac{2\pi i}{3}))} S(\theta). \quad (2.28)$$

The poles and zeroes of these two functions which can appear in the physical strip for  $0 < \lambda < 3$  are summarised in tables 1 and 2. Note that  $e^{\mathcal{A}(\theta)}$  has no physical strip poles at all for  $\lambda \leq 1$ .

For the critical models,  $\gamma$  lies between 0 and  $\pi/2$  and so the S-matrix parameter  $\lambda = 3\gamma/\pi$  should be between 0 and  $3/2$ . As mentioned above, the exponents of the tricritical models can be obtained by a continuation of  $\gamma$  into the interval  $[\pi/2, \pi]$ , and it is natural to suppose that the same should hold at the level of S-matrices. This led Chim and Zamolodchikov to conjecture that the S-matrix elements (2.17) – (2.20) with  $\lambda$  in the range  $[3/2, 3]$  should correspond to the scaling tricritical models. Thus the general relation between  $q$  and  $\lambda$  is

$$\sqrt{q} = 2 \sin\left(\frac{\pi\lambda}{3}\right), \quad \text{where } \lambda \in \begin{cases} [0, 3/2] & \text{(perturbed critical models);} \\ [3/2, 3] & \text{(perturbed tricritical models).} \end{cases} \quad (2.29)$$



	Poles					Zeroes
$\frac{\theta}{i\pi} =$	$\frac{1}{\lambda} - \frac{1}{3}$	$\frac{1}{\lambda}$	$\frac{2}{\lambda} - \frac{1}{3}$	$\frac{2}{\lambda}$	$\frac{3}{\lambda} - \frac{1}{3}$	1
Physical strip?	$\lambda > \frac{3}{4}$	$\lambda > 1$	$\lambda > \frac{3}{2}$	$\lambda > 2$	$\lambda > \frac{9}{4}$	$\forall \lambda$

Table 1: Physical strip poles and zeroes of  $e^{\mathcal{A}(\theta)}$ , for  $0 < \lambda < 3$

	Poles				Zeroes
$\frac{\theta}{i\pi} =$	$\frac{1}{3}$	$\frac{1}{\lambda}$	$\frac{1}{\lambda} + \frac{1}{3}$	$\frac{2}{\lambda}$	1
Physical strip?	$\forall \lambda$	$\lambda > 1$	$\lambda > \frac{3}{2}$	$\lambda > 2$	$\forall \lambda$

Table 2: Physical strip poles and zeroes of  $S(\theta)$ , for  $0 < \lambda < 3$

Recall that  $\lambda \in [0, 3/2]$  corresponds to  $\phi_{21}$  perturbations, and  $\lambda \in [3/2, 3]$  to  $\phi_{12}$ . In all cases the central charge of the unperturbed theory is

$$c = 1 - \frac{(3-2\lambda)^2}{(3+2\lambda)}. \quad (2.30)$$

For future reference, we also record the rational values of  $\lambda$ , following from (2.7) and (2.8) and the relation  $\lambda = \frac{3}{2}(\xi-1)/(\xi+1)$ , at which the off-critical Potts models are related to  $\phi_{21}$  and  $\phi_{12}$  perturbed minimal models  $\mathcal{M}_{pp'}$ ,  $p' > p$ :

$$\lambda = \frac{3p}{p'} - \frac{3}{2} \quad (\phi_{21} \text{ perturbations}); \quad (2.31)$$

$$\lambda = \frac{3p'}{p} - \frac{3}{2} \quad (\phi_{12} \text{ perturbations}). \quad (2.32)$$

### 3 Completing the bootstrap for $0 \leq \lambda \leq 3/2$

We now return to the discussion of the pole structures of the S-matrix elements, in order to see if there is any need to introduce further one-particle asymptotic states into the model, beyond the elementary kinks. It is convenient to phrase the discussion in terms of the variable

$$t = \frac{\theta}{i\pi} \quad (3.1)$$

already used implicitly in tables 1 and 2, so that the segment of the imaginary  $\theta$ -axis lying in the physical strip corresponds to real values of  $t$  between 0 and 1.  $t$  will sometimes be referred to as an ‘angle’, though strictly speaking the term should be

	Poles: $t =$			Poles: $t =$			Poles: $t =$	
$\mathcal{S}^0(\theta):$	$\frac{2}{3}$	$\frac{1}{3}$	$\mathcal{S}^1(\theta):$	$\frac{2}{3}$	$\mathcal{S}^2(\theta):$	$\frac{1}{3}$		
	$\frac{2}{3} - \frac{1}{\lambda}$	$\frac{1}{3} + \frac{1}{\lambda}$		$\frac{2}{3} - \frac{1}{\lambda}$		$\frac{1}{3} + \frac{1}{\lambda}$		
$\mathcal{S}^3(\theta):$	$\frac{1}{\lambda}$	$1 - \frac{1}{\lambda}$		$\frac{1}{\lambda}$		$1 - \frac{1}{\lambda}$		
	$\frac{2}{\lambda}$	$1 - \frac{2}{\lambda}$		$\frac{2}{\lambda}$		$1 - \frac{2}{\lambda}$		

Table 3: Physical strip poles of  $\mathcal{S}^0$ ,  $\mathcal{S}^1$ ,  $\mathcal{S}^2$  and  $\mathcal{S}^3$  for  $0 \leq \lambda \leq 3$

reserved for  $\pi t$  rather than  $t$ . The poles at  $t = 2/3$  in  $\mathcal{S}^0$  and  $\mathcal{S}^1$ , and at  $t = 1/3$  in  $\mathcal{S}^0$  and  $\mathcal{S}^2$ , have already been treated, and are due to the fundamental kink itself. In [1], Chim and Zamolodchikov noted that extra poles enter the physical strip once  $\lambda$  passes 1. These they assigned to a new particle  $B$ , a breather-like excitation over a single vacuum, appearing as a bound state in the scattering of two kinks. The associated S-matrix elements  $\mathcal{S}_{BK}$  and  $\mathcal{S}_{BB}$  also contain physical strip poles. Some of these correspond to the kink and breather already seen, but others were conjectured in [1] to signal the presence of yet further particles. In this section, we re-examine this analysis and find that these further particles do not in fact appear in the spectrum while the critical models are considered. The range  $3/2 < \lambda \leq 3$ , corresponding to perturbations of the tricritical models, turns out to be far more complicated and we postpone its discussion until section 4.

### 3.1 The pole structure of the fundamental kink amplitudes

Table 3 summarises the physical strip pole structure of the fundamental amplitudes (2.17)-(2.20), for  $\lambda$  in the range  $0 \leq \lambda \leq 3$ . Supposing each pole to correspond to a bound state particle in either the direct or the crossed channel, a consideration of the patterns of vacua shown in figure 1 allows them to be classified as follows. All four vacua seen by  $\mathcal{S}^0$  are different, so all of its poles must correspond to kink type particles. One out of each pair of poles in  $\mathcal{S}^0$  appears in  $\mathcal{S}^1$ , and the other in  $\mathcal{S}^2$ . To be consistent with the vacuum structure, the pole also appearing in  $\mathcal{S}^1$  must be direct channel, and that also in  $\mathcal{S}^2$  cross channel. Similarly, all poles in  $\mathcal{S}^3$  must correspond to excitations over a single vacuum (breathers). All poles which also appear in  $\mathcal{S}^2$  must be direct channel, while those which also appear in  $\mathcal{S}^1$  must be cross channel. The resulting particle spectrum is summarised in table 4, and the corresponding fusing vertices are

Pole: $t =$	$\frac{2}{3}$	$\frac{2}{3} - \frac{1}{\lambda}$	$1 - \frac{1}{\lambda}$	$1 - \frac{2}{\lambda}$
Physical strip?	$\forall \lambda$	$\lambda > \frac{3}{2}$	$\lambda > 1$	$\lambda > 2$
Mass:	$m$	$2m \cos\left(\frac{\pi}{3} - \frac{\pi}{2\lambda}\right)$	$2m \cos\left(\frac{\pi}{2} - \frac{\pi}{2\lambda}\right)$	$2m \cos\left(\frac{\pi}{2} - \frac{\pi}{\lambda}\right)$
Particle:	$K_1 (= K)$	$K_2$	$B_1 (= B)$	$B_2$

Table 4: Direct channel pole assignments for  $\mathcal{S}^0$ ,  $\mathcal{S}^1$ ,  $\mathcal{S}^2$  and  $\mathcal{S}^3$

depicted in figure 5.

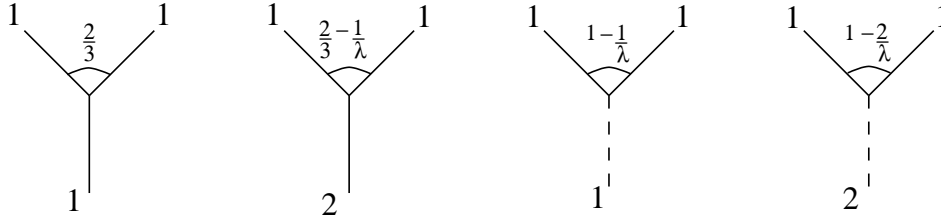


Figure 5:  $K_1 K_1$  fusing vertices

Restricting to the range  $0 \leq \lambda \leq 3/2$ , the only bound states signalled in  $K_1 K_1$  scattering are the fundamental kink  $K_1$  itself, and, for  $1 < \lambda \leq 3/2$ , the breather  $B_1$ .

### 3.2 Two particles: $1 < \lambda \leq 3/2$

For  $\lambda \leq 1$ , the bootstrap closes on the fundamental kink alone and there is no more to be done, but once  $\lambda$  increases beyond 1 the breather  $B_1$  appears. This extra particle brings with it two new scattering amplitudes,  $\mathcal{S}_{B_1 K_1}$  and  $\mathcal{S}_{B_1 B_1}$ :

$$\mathcal{S}_{B_1 K_1} = \left[\frac{1}{2} + \frac{1}{2\lambda}\right] \left[\frac{1}{6} + \frac{1}{2\lambda}\right], \quad (3.2)$$

$$\mathcal{S}_{B_1 B_1} = \left[\frac{2}{3}\right] \left[\frac{1}{\lambda}\right] \left[\frac{1}{\lambda} - \frac{1}{3}\right]. \quad (3.3)$$

Here we have rewritten the formulae from [1] using the blocks

$$[a] = (a)(1 - a), \quad \text{where} \quad (a) = \frac{\sinh\left(\frac{\theta}{2} + \frac{i\pi a}{2}\right)}{\sinh\left(\frac{\theta}{2} - \frac{i\pi a}{2}\right)}. \quad (3.4)$$

The new amplitudes are illustrated in figure 6.



Figure 6:  $B_1K_1 \rightarrow K_1B_1$  and  $B_1B_1 \rightarrow B_1B_1$  scattering

The pole structures of these new S-matrix elements must be examined to see if there are any further bound states. It is at this stage that our analysis diverges from that of [1], since it turns out that variants of the Coleman-Thun mechanism [15] allow some poles to be explained, for certain ranges of  $\lambda$ , without the need to introduce new particles. We shall treat the two new amplitudes in turn.

### 3.3 The $B_1K_1$ scattering amplitude

The relevant S-matrix element, which is also depicted in appendix D, is

$$\mathcal{S}_{B_1K_1} = [\frac{1}{2} + \frac{1}{2\lambda}][\frac{1}{6} + \frac{1}{2\lambda}] = (\frac{1}{2} - \frac{1}{2\lambda})(\frac{1}{2} + \frac{1}{2\lambda})(\frac{1}{6} + \frac{1}{2\lambda})(\frac{5}{6} - \frac{1}{2\lambda}) \quad (3.5)$$

The  $K_1K_1B_1$  vertex allows the poles from the factors  $(\frac{1}{2} + \frac{1}{2\lambda})$  and  $(\frac{1}{2} - \frac{1}{2\lambda})$  to be identified with the original kink  $K_1$  appearing as a bound state in the direct and crossed channels respectively. Assuming that the poles in  $[\frac{1}{6} + \frac{1}{2\lambda}]$  also correspond to a bound state, we make an initial hypothesis that the direct channel pole is at  $t = \frac{1}{6} + \frac{1}{2\lambda}$ . The associated particle must be an excited kink of some sort, and calculating its mass we find

$$m = 2m \cos(\frac{\pi}{3} - \frac{1}{2\lambda}) . \quad (3.6)$$

Comparing with the masses listed in table 4, it is natural to identify this with the  $K_2$  state already seen in  $K_1K_1$  scattering. This implies the existence of a vertex coupling  $K_1$ ,  $K_2$  and  $B_1$ , and the corresponding fusing angles are shown in figure 7.

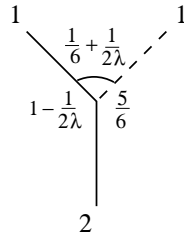


Figure 7: the  $K_1B_1 \rightarrow K_2$  vertex

Unlike the  $K_2$  bound state poles in  $\mathcal{S}^0$  and  $\mathcal{S}^1$ , which only enter the physical strip for  $\lambda > \frac{3}{2}$ , the  $(\frac{5}{6} - \frac{1}{2\lambda})(\frac{1}{6} + \frac{1}{2\lambda})$  poles in  $\mathcal{S}_{B_1 K_1}$  are already in the physical strip at  $\lambda = 1$ . This suggests that  $K_2$  should be present in the particle spectrum for all  $\lambda > 1$ , and indeed this was proposed in [1]. We would like to advocate an alternative scenario, which begins with the observation that, for  $\lambda < 3/2$ , one would expect the  $B_1 K_1$  scattering amplitude to exhibit an anomalous threshold pole exactly at the location of the would-be  $K_2$  bound state pole, since the on-shell diagram shown in figure 8 is geometrically possible.

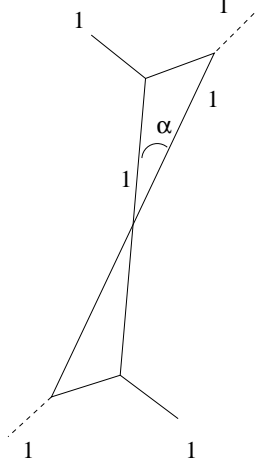


Figure 8:  $K_1 B_1$  scattering: the pole at  $t = \frac{1}{6} + \frac{1}{2\lambda}$ , for  $\lambda < \frac{3}{2}$

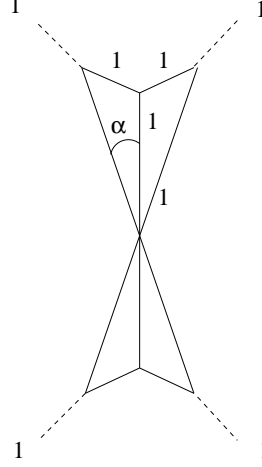


Figure 9:  $B_1 B_1$  scattering: the pole at  $t = \frac{1}{\lambda} - \frac{1}{3}$ , for  $\lambda < \frac{3}{2}$

The angle between the incoming particles  $K_1$  and  $B_1$  is  $t = \frac{1}{6} + \frac{1}{2\lambda}$ , and the internal scattering angle is  $\alpha = \frac{1}{\lambda} - \frac{2}{3}$ . The diagram closes for  $0 < \alpha < \frac{1}{3}$ , which translates as  $1 < \lambda < \frac{3}{2}$ . However, in two dimensions a diagram of this sort would usually be expected to give rise to a double pole, while  $\mathcal{S}_{B_1 K_1}$  only has a simple pole at this value of  $t$ . The problem is resolved once the contributions of the couplings and S-matrix elements are taken into account. These are composed of four three-particle couplings multiplying a sum over two-particle amplitudes. This sum, which we shall denote by  $\mathcal{C}$ , can be computed by considering the possibilities for the internal vacua in the diagram. The ‘upper’ internal vacuum must differ from both external vacua, and so can take  $(q-2)$  values. Once this vacuum has been fixed, there are again  $(q-2)$  possibilities for the lower internal vacuum, but they are no longer equivalent. Either the lower vacuum is equal to the upper one (1 possibility), in which case the relevant two-particle amplitude needed to evaluate the diagram is  $\mathcal{S}^1(i\pi\alpha)$ , or else it is different ( $(q-3)$  possibilities), in which case the amplitude is rather  $\mathcal{S}^0(i\pi\alpha)$ . Adding everything up, we have

$$\begin{aligned} \mathcal{C} &= (q-2) [\mathcal{S}^1(i\pi\alpha) + (q-3)\mathcal{S}^0(i\pi\alpha)] \\ &= \frac{(q-2)\mathcal{S}(i\pi\alpha)}{\sin((\frac{2}{3}-\alpha)\pi\lambda)\sin(\frac{\pi}{3}\lambda)} [\sin(\frac{2\pi}{3}\lambda)\sin((\frac{1}{3}-\alpha)\pi\lambda) + \sin(\pi\lambda)\sin(\alpha\pi\lambda)] \end{aligned} \quad (3.7)$$

where use has been made of equation (2.29). Substituting  $\alpha = \frac{1}{\lambda} - \frac{2}{3}$ , and noting that  $S(i\pi\alpha)$  does not have any poles or zeroes at this value of  $\alpha$ , reveals a remarkable cancellation:

$$\mathcal{C} = -\frac{(q-2)S(i\pi\alpha)}{\sin(\frac{4\pi}{3}\lambda)\sin(\pi\lambda)}[-\sin(\frac{2\pi}{3}\lambda)\sin(\pi\lambda) + \sin(\pi\lambda)\sin(\frac{2\pi}{3}\lambda)] = 0. \quad (3.8)$$

The vanishing of  $\mathcal{C}$  reduces the overall singularity associated with the diagram to a simple pole. Thus the pole at  $t = \frac{1}{6} + \frac{1}{2\lambda}$  in  $\mathcal{S}_{B_1K_1}$  can be explained without the need to introduce the excited kink  $K_2$ , at least until  $\lambda = \frac{3}{2}$ . Beyond this point, the scattering process shown in figure 8 is no longer geometrically possible; and at the same time, the presence of  $K_2$  in the spectrum is also signalled by the appearance of its bound state pole in the kink-kink matrix elements  $\mathcal{S}^0$  and  $\mathcal{S}^1$ .

A very similar phenomenon was observed many years ago by Coleman and Thun in the Sine-Gordon model [15], where the appearance of new breathers is delayed until their poles are seen in the soliton-soliton S-matrix (see section 4 of [16] for a detailed review of this story). It has also played a rôle in the understanding of non self-dual affine Toda field theories [17], and crops up in the analysis of boundary scattering [18]. A novel feature here is the formal treatment of the vacua. When working out the combinatorics,  $q$  is treated as an integer, and the resulting formula is then taken to hold for general  $q$ . The same spirit guided Chim and Zamolodchikov's original formulation of the Yang-Baxter equations for the model; it can be interpreted as a way to account for the statistics of the kink states in a way that depends smoothly on  $q$ . In principle it should be possible to phrase the discussion entirely within the more standardly-defined formulation of Smirnov [2], but since in this approach the vacuum structure depends in a discontinuous way on  $q$ , the arguments are likely to be considerably more involved.

### 3.4 The $B_1B_1$ scattering amplitude

To complete the analysis we must consider

$$\mathcal{S}_{B_1B_1} = [\frac{2}{3}][\frac{1}{\lambda}][\frac{1}{\lambda} - \frac{1}{3}] = (\frac{1}{3})(\frac{2}{3})(\frac{1}{\lambda})(1 - \frac{1}{\lambda})(\frac{1}{\lambda} - \frac{1}{3})(\frac{2}{3} - \frac{1}{\lambda}). \quad (3.9)$$

The poles from the blocks  $(\frac{2}{3})$  and  $(\frac{1}{3})$  can be identified with  $B_1$  bound states in the direct and cross channels respectively. The poles from  $(\frac{1}{\lambda})$  and  $(1 - \frac{1}{\lambda})$  match direct and cross channel bound states of  $B_2$ , while that in  $(\frac{1}{\lambda} - \frac{1}{3})$  is potentially the direct channel pole for a new particle,  $B_3$ , with mass

$$m_{B_3} = 2m_{B_1} \cos(\frac{\pi}{2\lambda} - \frac{\pi}{6}) = 4m \cos(\frac{\pi}{2} - \frac{\pi}{2\lambda}) \cos(\frac{\pi}{2\lambda} - \frac{\pi}{6}). \quad (3.10)$$

(This particle was denoted  $B'$  in [1].) The poles at  $\frac{1}{\lambda}$  and  $\frac{1}{\lambda} - \frac{1}{3}$  are both located in the physical strip for  $\lambda > 1$ , when  $B_1$  first appears.

However, the appearance of both  $B_2$  and  $B_3$  can be delayed by invoking the Coleman-Thun mechanism. Most complicated to treat is the would-be  $B_3$  bound state pole. The a-priori third order diagram shown in figure 9 has internal scattering angle  $\alpha = \frac{1}{\lambda} - \frac{2}{3}$ ,

and thus closes for  $\lambda < \frac{3}{2}$ . Keeping track of all possible combinations we find that the third-order pole must be multiplied by a factor

$$\mathcal{C} = (q-1)(q-2) [\mathcal{S}^1(i\pi\alpha) + (q-3)\mathcal{S}^0(i\pi\alpha)]^2 [\mathcal{S}^1(i2\pi\alpha) + (q-3)\mathcal{S}^0(i2\pi\alpha)]. \quad (3.11)$$

We have already seen that  $\mathcal{S}^1(i\pi\alpha) + (q-3)\mathcal{S}^0(i\pi\alpha) = 0$  for  $\alpha = \frac{1}{\lambda} - \frac{2}{3}$  in the treatment of  $\mathcal{S}_{B_1 K_1}$ , and a simple calculation shows that the rest of the function is finite and non-zero at this point. The diagram thus contributes a simple pole, and  $B_3$  need not show up as a bound state until  $\lambda = \frac{3}{2}$ .

Turning to the pole at  $t = \frac{1}{\lambda}$ , provisionally assigned to  $B_2$ , the relevant diagram is shown in figure 10. The internal scattering angle  $\alpha = \frac{2}{\lambda} - 1$  is positive (making the diagram geometrically possible) for  $\lambda < 2$ . Calculating the prefactor  $\mathcal{C}$  we have

$$\begin{aligned} \mathcal{C} &= (q-1) [\mathcal{S}^3(i\pi\alpha) + (q-2)\mathcal{S}_1(i\pi\alpha)] \\ &= (q-1) \frac{\sin((\alpha - \frac{1}{3})\pi\lambda) \mathcal{S}(i\pi\alpha)}{\sin(\frac{\pi}{3}\lambda)} \left[ \frac{\sin(\pi\lambda)}{\sin((\alpha-1)\pi\lambda)} + (q-2) \frac{\sin(\frac{2\pi}{3}\lambda)}{\sin((\alpha - \frac{2}{3})\pi\lambda)} \right]. \end{aligned} \quad (3.12)$$

At  $\alpha = \frac{2}{\lambda} - 1$ , the expression in square brackets vanishes and the overall singularity is reduced from a double to a single pole. This means that there is no need to introduce the  $B_2$  breather until  $\lambda$  passes 2, at which stage it also appears in the  $K_1 K_1$  amplitudes  $\mathcal{S}^2$  and  $\mathcal{S}^3$ .

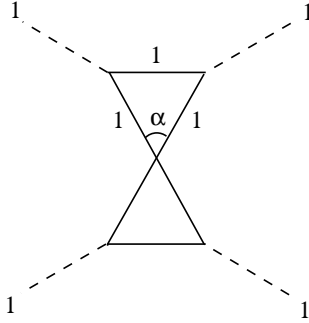


Figure 10:  $B_1 B_1$  scattering:  $t = \frac{1}{\lambda}$ ,  $\lambda < 2$

### 3.5 Checks on the spectrum for $0 < \lambda \leq 3/2$

To summarise, by invoking the Coleman-Thun mechanism we have seen that the only particles forced to appear for  $0 < \lambda < \frac{3}{2}$  are the fundamental kink  $K_1$ , present for all  $\lambda$ , and the breather  $B_1$ , which appears for  $\lambda > 1$ . The two bound states  $K_2$  and  $B_3$  proposed by Chim and Zamolodchikov need not appear until  $\lambda > \frac{3}{2}$ . We also saw evidence for a further new particle  $B_2$ , but its appearance was postponed until  $\lambda > 2$ .

While we have shown that our proposed spectrum is consistent, strictly speaking the larger spectrum initially suggested by Chim and Zamolodchikov has not been completely ruled out – genuine bound state poles could be hiding behind the contributions provided by the Coleman-Thun diagrams. Some reassurance comes from some work by Delfino

and Cardy [12]. They calculated a number of universal quantities using the form-factor approach, which is sensitive to the massive particle spectrum. Some of these quantities (for example the central charge) can be compared with known results. While the need to add in the first breather state at  $\lambda = 1$  is clearly signalled, the data up to  $\lambda = 3/2$ , as illustrated by figure 5 of [12], shows no signs of any further missing particles.

Another check comes from the limiting point  $\lambda = \frac{3}{2}$ ,  $q = 4$ , where the S-matrix for the minimal  $D_4$  related field theory discussed in [19] should be reproduced. The spectrum of this model consists of three light particles  $l$ ,  $l'$ ,  $l''$  with the same mass  $m_l$ , and one particle  $h$  of mass  $m_h = \sqrt{3}m_l$ . The mass ratio  $m_h : m_l$  equals that of  $m_{B_1} : m_{K_1}$ , and  $h$  is naturally identified with  $B_1$ . There are three distinct ways of pairing up the four vacua and each of these may be associated with one of the light particles. This is shown in figure 11, where for example  $l$  is identified with domain walls  $1 \leftrightarrow 2$  and  $3 \leftrightarrow 4$  (vacua labeled from 1 to 4). This identification is unique up to permutations of the light particles amongst themselves — also a property of the  $D_4$  S-matrix. The two-particle amplitudes  $\mathcal{S}_{ll}(\theta)$ ,  $\mathcal{S}_{l'l'}(\theta)$ ,  $\mathcal{S}_{l'l''}(\theta)$  and  $\mathcal{S}_{hh}(\theta)$  then correspond to  $\mathcal{S}^3(\theta)$ ,  $\mathcal{S}^0(\theta)$ ,  $\mathcal{S}_{B_1K_1}(\theta)$  and  $\mathcal{S}_{B_1B_1}(\theta)$  respectively. Substituting for  $\lambda$ , a direct comparison can be made with the results of [19]. The S-matrices match, since  $\mathcal{S}^1(\theta)$  and  $\mathcal{S}^2(\theta)$  vanish for  $\lambda = \frac{3}{2}$ . Notice that the set of spins of conserved charges for the  $D_4$ -related model starts 1, 3, 3, 5... and is thus larger than the generic  $\phi_{21}$  spectrum  $s = 1, 5, 7, 11 \dots$  reported above. Moving from the kink to the particle picture, the  $\phi^3$  property of the S-matrix is lost, and it is this which allows the enlarged set of conserved charges to be represented locally on the multiparticle states. In the kink basis, the extra charges are also present for  $\lambda = 3/2$ , but they do not act diagonally.

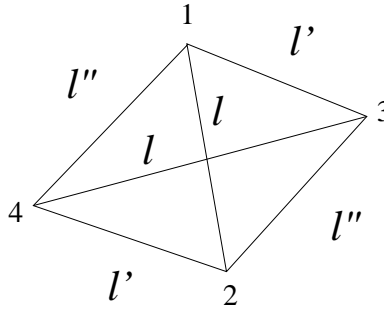


Figure 11: Domain walls  $\leftrightarrow$  particles at  $q = 4$

#### 4 Perturbed tricritical models: $3/2 < \lambda < 3$

We now move to the region  $\frac{3}{2} \leq \lambda \leq 3$ , suggested in [1] to describe the scaling tricritical  $q$ -state Potts models, and related to  $\phi_{12}$  perturbations of  $c < 1$  conformal field theories. The full S-matrix becomes extremely complicated as  $\lambda$  increases, and we have not completed our analysis for the whole tricritical range of  $\lambda$ . For this reason we will be a little more sketchy in our descriptions in this section. Some further details are in the appendices, and in [20].



#### 4.1 Four particles: $3/2 < \lambda \leq 2$

Two new particles,  $K_2$  and  $B_3$ , must appear once  $\lambda$  passes  $\frac{3}{2}$ . We found that no further particles were needed to explain the pole structure up to  $\lambda = 2$ . The new S-matrix elements are as follows:

$$\begin{aligned}
\mathcal{S}_{K_1 K_2}^a &= t\left(\frac{1}{3} + \frac{1}{2\lambda}\right)t\left(\frac{1}{3} - \frac{1}{2\lambda}\right)t\left(\frac{1}{2\lambda}\right)t\left(\frac{2}{3} - \frac{1}{2\lambda}\right)\mathcal{S}^a\left(\theta + \frac{i\pi}{2\lambda}\right) \\
\mathcal{S}_{K_2 K_2}^a &= \left[\frac{2}{3}\right]^2\left[\frac{1}{3} + \frac{1}{\lambda}\right]\left[\frac{1}{\lambda}\right]\mathcal{S}^a \\
\mathcal{S}_{B_1 K_2} &= \left[\frac{1}{2}\right]\left[\frac{5}{6}\right]\left[\frac{1}{6} + \frac{1}{\lambda}\right]\left[\frac{1}{\lambda} - \frac{1}{6}\right] \\
\mathcal{S}_{B_3 K_1} &= \left[\frac{1}{3}\right]^2\left[\frac{1}{\lambda}\right]\left[\frac{1}{\lambda} + \frac{1}{3}\right] \\
\mathcal{S}_{B_3 K_2} &= \left[1 - \frac{1}{2\lambda}\right]^2\left[\frac{1}{3} + \frac{1}{2\lambda}\right]^3\left[\frac{2}{3} + \frac{1}{2\lambda}\right]\left[\frac{3}{2\lambda} - \frac{1}{3}\right]\left[\frac{3}{2\lambda}\right] \\
\mathcal{S}_{B_3 B_3} &= \left[\frac{2}{3}\right]^3\left[\frac{1}{\lambda}\right]^3\left[\frac{4}{3} - \frac{1}{\lambda}\right]^2\left[\frac{1}{3} + \frac{1}{\lambda}\right]\left[\frac{2}{\lambda} - \frac{2}{3}\right]\left[\frac{2}{\lambda} - \frac{1}{3}\right] \\
\mathcal{S}_{B_3 B_1} &= \left[\frac{1}{6} + \frac{1}{2\lambda}\right]^2\left[\frac{1}{2} + \frac{1}{2\lambda}\right]\left[\frac{7}{6} - \frac{1}{2\lambda}\right]\left[\frac{3}{2\lambda} - \frac{1}{2}\right]\left[\frac{3}{2\lambda} - \frac{1}{6}\right]
\end{aligned} \tag{4.1}$$

where  $t(a)(t) = \tan\left(\frac{\pi}{2}(t + a)\right)$ , the blocks  $[a]$  were defined in equation (3.4) above, and  $\mathcal{S}^a$  are the amplitudes for the scattering of the fundamental kink  $K_1$ . (Note the shift in the argument in the first formula.) Once again there are four possible amplitudes corresponding to the four different vacuum structures for kink-kink scattering. In tables 5 and 6 we summarise the physical-strip poles of the new kink-kink amplitudes for  $3/2 < \lambda \leq 3$ .

The introduction of new particles leads to further bootstrap equations. Here we quickly sketch those for the new kink-kink amplitudes.  $K_2$  appears as a bound state in  $K_1 K_1$ ,  $K_1 B_1$ , and  $K_1 B_3$  scattering. This allows  $\mathcal{S}_{K_1 K_2}^a$  to be obtained via a number of a-priori distinct bootstrap equations. Consider first the  $K_1 K_1 \rightarrow K_2$  fusing. The general kink bootstrap equation illustrated in figure 4 implies

$$\mathcal{S}_{K_1 K_2}^a(\theta) = \sum \mathcal{S}_{K_1 K_1}(\theta - \frac{i\pi}{3} + \frac{i\pi}{2\lambda})\mathcal{S}_{K_1 K_1}(\theta + \frac{i\pi}{3} - \frac{i\pi}{2\lambda}) \tag{4.2}$$

where the terms to be summed on the right-hand side depend both on the particular matrix element being evaluated, and on the choice of vacuum  $b$  in figure 4. For example:

$$\begin{aligned}
\mathcal{S}_{K_1 K_2}^0(\theta) &= \mathcal{S}^3\mathcal{S}^0 + \mathcal{S}^2\mathcal{S}^2 + (q - 4)\mathcal{S}^2\mathcal{S}^0 \\
&= \mathcal{S}^1\mathcal{S}^1 + \mathcal{S}^0\mathcal{S}^3 + (q - 4)\mathcal{S}^0\mathcal{S}^1 \\
&= \mathcal{S}^1\mathcal{S}^0 + \mathcal{S}^0\mathcal{S}^2 + (q - 5)\mathcal{S}^0\mathcal{S}^0.
\end{aligned} \tag{4.3}$$

The compatibility of these formulae provides constraints on the non-scalar parts of the  $K_1 K_1$  amplitudes, which turn out to be just the original bootstrap equations, with  $\theta$  shifted by  $\frac{i\pi}{2\lambda}$ .

Alternatively, the  $K_1 K_2$  scattering amplitude could have been found using either the  $K_1 B_1 \rightarrow K_2$  fusing:

$$\begin{aligned}
\mathcal{S}_{K_1 K_2}^a(\theta) &= \mathcal{S}_{K_1 B_1}(\theta - \frac{i\pi}{6})\mathcal{S}_{K_1 K_1}^a(\theta + \frac{i\pi}{2\lambda}) \\
&= \mathcal{S}_{K_1 B_1}(\theta + \frac{i\pi}{6})\mathcal{S}_{K_1 K_1}^a(\theta - \frac{i\pi}{2\lambda})
\end{aligned} \tag{4.4}$$

$t = \theta/i\pi$	Poles: $t =$					
$\mathcal{S}_{K_2K_1}^0(\theta) :$	$\frac{2}{3} + \frac{1}{2\lambda}$ $\frac{1}{3} - \frac{1}{2\lambda}$	$(\frac{1}{3} + \frac{1}{2\lambda})^2$ $(\frac{2}{3} - \frac{1}{2\lambda})^2$	$\frac{2}{3} - \frac{3}{2\lambda}$ $\frac{1}{3} + \frac{3}{2\lambda}$			
$\mathcal{S}_{K_2K_1}^1(\theta) :$	$\frac{2}{3} + \frac{1}{2\lambda}$	$\frac{1}{3} + \frac{1}{2\lambda}$ $(\frac{2}{3} - \frac{1}{2\lambda})^2$	$\frac{2}{3} - \frac{3}{2\lambda}$	$\frac{1}{2\lambda}$	$\frac{3}{2\lambda}$	$\frac{5}{2\lambda}$
$\mathcal{S}_{K_2K_1}^2(\theta) :$	$\frac{1}{3} - \frac{1}{2\lambda}$	$(\frac{1}{3} + \frac{1}{2\lambda})^2$ $\frac{2}{3} - \frac{1}{2\lambda}$	$\frac{1}{3} + \frac{3}{2\lambda}$	$1 - \frac{1}{2\lambda}$	$1 - \frac{3}{2\lambda}$	$1 - \frac{5}{2\lambda}$
$\mathcal{S}_{K_2K_1}^3(\theta) :$		$\frac{1}{3} + \frac{1}{2\lambda}$ $\frac{2}{3} - \frac{1}{2\lambda}$		$1 - \frac{1}{2\lambda}$ $\frac{1}{2\lambda}$	$1 - \frac{3}{2\lambda}$ $\frac{3}{2\lambda}$	$1 - \frac{5}{2\lambda}$ $\frac{5}{2\lambda}$

Table 5: Physical strip poles of  $\mathcal{S}_{K_1K_2}^0$ ,  $\mathcal{S}_{K_1K_2}^1$ ,  $\mathcal{S}_{K_1K_2}^2$  and  $\mathcal{S}_{K_1K_2}^3$  for  $3/2 < \lambda \leq 3$

or the  $K_1 B_3 \rightarrow K_2$  fusing:

$$\begin{aligned}
\mathcal{S}_{K_1K_2}^a(\theta) &= \mathcal{S}_{K_1B_3}(\theta - \frac{i\pi}{3} + \frac{i\pi}{2\lambda})\mathcal{S}_{K_1K_1}^a(\theta + \frac{3\pi i}{2\lambda}) \\
&= \mathcal{S}_{K_1B_3}(\theta + \frac{i\pi}{3} - \frac{i\pi}{2\lambda})\mathcal{S}_{K_1K_1}^a(\theta - \frac{3\pi i}{2\lambda}).
\end{aligned} \tag{4.5}$$

The equality of the two expressions in (4.4) can be checked using

$$S(\theta + \frac{i\pi}{\lambda}) = -\frac{\sinh(\frac{\theta}{2} - \frac{i\pi}{2})\sinh(\frac{\theta}{2} - \frac{i\pi}{2} + \frac{i\pi}{2\lambda})\sinh(\frac{\theta}{2} - \frac{i\pi}{3})\sinh(\frac{\theta}{2} + \frac{i\pi}{3} + \frac{i\pi}{2\lambda})}{\sinh(\frac{\theta}{2})\sinh(\frac{\theta}{2} + \frac{i\pi}{2\lambda})\sinh(\frac{\theta}{2} + \frac{i\pi}{6})\sinh(\frac{\theta}{2} - \frac{i\pi}{6} + \frac{i\pi}{2\lambda})} S(\theta). \tag{4.6}$$

Then (4.5) can be rewritten in a form that can more easily be compared with (4.4) by making use of (4.6) and the fact that

$$\mathcal{S}_{K_1K_1}^a(\theta \pm \frac{i\pi}{\lambda}) = \frac{S(\theta \pm \frac{i\pi}{\lambda})}{S(\theta)} \mathcal{S}_{K_1K_1}^a(\theta). \tag{4.7}$$

As a last step, we need to check the compatibility of (4.4) with (4.2). Starting from (4.2) we can use (4.7) and (4.6) to rewrite each  $\mathcal{S}_{K_1K_1}(\theta + \frac{i\pi}{3} - \frac{i\pi}{2\lambda})$  as  $\mathcal{S}_{K_1K_1}(\theta + \frac{i\pi}{3} + \frac{i\pi}{2\lambda})$  multiplied by a common factor. The non-scalar parts of the formula are then the original

$t = \theta/i\pi$	Poles: $t =$			
$\mathcal{S}_{K_2K_2}^0(\theta) :$	$(\frac{2}{3})^3$	$(\frac{1}{3})^3$	$\mathcal{S}_{K_2K_2}^1(\theta) :$	$(\frac{2}{3})^3$ $(\frac{1}{3})^2$
	$(\frac{2}{3} - \frac{1}{\lambda})^2$	$(\frac{1}{3} + \frac{1}{\lambda})^2$		$(\frac{2}{3} - \frac{1}{\lambda})^2$ $\frac{1}{3} + \frac{1}{\lambda}$
	$1 - \frac{1}{\lambda}$	$\frac{1}{\lambda}$		$1 - \frac{1}{\lambda}$ $(\frac{1}{\lambda})^2$
				$\frac{2}{\lambda}$
$\mathcal{S}_{K_2K_2}^2(\theta) :$	$(\frac{2}{3})^2$	$(\frac{1}{3})^3$	$\mathcal{S}_{K_2K_2}^3(\theta) :$	$(\frac{2}{3})^2$ $(\frac{1}{3})^2$
	$\frac{2}{3} - \frac{1}{\lambda}$	$(\frac{1}{3} + \frac{1}{\lambda})^2$		$\frac{2}{3} - \frac{1}{\lambda}$ $\frac{1}{3} + \frac{1}{\lambda}$
	$(1 - \frac{1}{\lambda})^2$	$\frac{1}{\lambda}$		$(1 - \frac{1}{\lambda})^2$ $(\frac{1}{\lambda})^2$
		$1 - \frac{2}{\lambda}$		$1 - \frac{2}{\lambda}$ $\frac{2}{\lambda}$

Table 6: Physical strip poles of  $\mathcal{S}_{K_2K_2}^0$ ,  $\mathcal{S}_{K_2K_2}^1$ ,  $\mathcal{S}_{K_2K_2}^2$  and  $\mathcal{S}_{K_2K_2}^3$  for  $3/2 < \lambda \leq 3$

bootstrap equations for  $\mathcal{S}_{K_1K_1}^a(\theta + \frac{i\pi}{2\lambda})$ , leaving it to be checked that the extra factor is equal to  $\mathcal{S}_{K_1B_1}(\theta - \frac{i\pi}{6})$ . The bootstrap equations for  $\mathcal{S}_{K_2K_2}^a(\theta)$  can be treated in a similar manner, and all are found to be satisfied.

While we omit the full details here, we have checked that, for  $3/2 < \lambda < 2$ , all poles in the S-matrix elements have a potential field-theoretical explanation, often via quite elaborate incarnations of the Coleman-Thun mechanism. To give just one example, the triple pole in  $\mathcal{S}_{B_3B_3}$  at  $t = \frac{1}{\lambda}$  can be associated with the diagram shown in figure 12, which closes for  $\frac{3}{2} < \lambda < \frac{9}{4}$ . The fusing angles needed to verify that the diagram does indeed close as claimed can be found in appendix B.

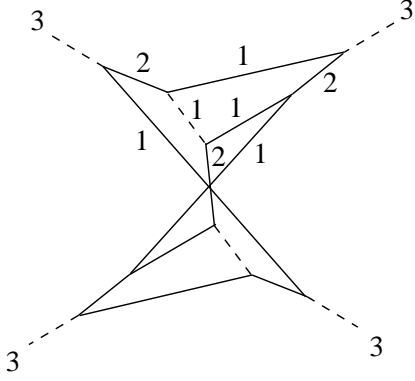


Figure 12:  $B_3 B_3$  scattering: the triple pole at  $t = \frac{1}{\lambda}$ , for  $\frac{3}{2} < \lambda < \frac{9}{4}$

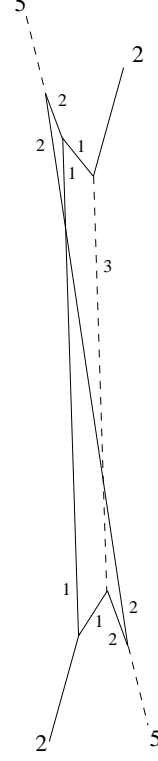


Figure 13:  $B_5 K_2$  scattering: the double pole at  $t = \frac{1}{6}$ , for  $2 < \lambda < \frac{9}{4}$

## 4.2 Six particles: $2 < \lambda \leq 9/4$

For  $2 < \lambda < \frac{9}{4}$ , the already-advertised  $B_2$  together with a further breather  $B_5$  enter the spectrum. The scattering amplitudes for the new particles become increasingly complicated, and greater reliance must be placed on the Coleman-Thun mechanism to explain the pole structure. The new S-matrix elements in this region are:

$$\begin{aligned}
\mathcal{S}_{B_2 B_1} &= [1 - \frac{1}{2\lambda}][\frac{2}{3} - \frac{1}{2\lambda}][\frac{3}{2\lambda}][\frac{3}{2\lambda} - \frac{1}{3}] \\
\mathcal{S}_{B_2 B_2} &= [\frac{2}{3}][\frac{2}{3} - \frac{1}{\lambda}][\frac{1}{\lambda} - \frac{1}{3}][\frac{2}{\lambda}][\frac{2}{\lambda} - \frac{1}{3}][1 - \frac{1}{\lambda}]^2 \\
\mathcal{S}_{B_2 B_3} &= [\frac{1}{2}][\frac{5}{6}][\frac{2}{\lambda} - \frac{1}{6}][\frac{7}{6} - \frac{1}{\lambda}]^2[\frac{2}{\lambda} - \frac{1}{2}][\frac{5}{6} - \frac{1}{\lambda}]^2 \\
\mathcal{S}_{B_2 K_1} &= [\frac{1}{2}][\frac{1}{6}][\frac{1}{2} + \frac{1}{\lambda}][\frac{1}{6} + \frac{1}{\lambda}] \\
\mathcal{S}_{B_2 K_2} &= [\frac{1}{2} - \frac{1}{2\lambda}]^2[\frac{1}{6} + \frac{1}{2\lambda}]^2[\frac{1}{6} + \frac{3}{2\lambda}][\frac{3}{2\lambda} - \frac{1}{6}] \\
\mathcal{S}_{B_5 B_1} &= [\frac{1}{3}]^2[\frac{4}{3} - \frac{1}{\lambda}][\frac{1}{3} + \frac{1}{\lambda}][\frac{2}{\lambda} - \frac{2}{3}][\frac{2}{\lambda} - \frac{1}{3}][1 - \frac{1}{\lambda}]^2 \\
\mathcal{S}_{B_5 B_2} &= [\frac{4}{3} - \frac{3}{2\lambda}]^2[1 - \frac{3}{2\lambda}]^2[\frac{2}{3} + \frac{1}{2\lambda}][\frac{1}{3} + \frac{1}{2\lambda}][1 - \frac{1}{2\lambda}]^2[\frac{5}{2\lambda} - \frac{1}{3}][\frac{5}{2\lambda} - \frac{2}{3}] \\
\mathcal{S}_{B_5 B_3} &= [\frac{7}{6} - \frac{1}{2\lambda}][\frac{1}{6} + \frac{3}{2\lambda}][\frac{3}{2} - \frac{3}{2\lambda}]^2[\frac{5}{2\lambda} - \frac{5}{6}][\frac{1}{2} + \frac{1}{2\lambda}]^3[\frac{3}{2\lambda} - \frac{1}{6}]^3[\frac{5}{2\lambda} - \frac{1}{2}][\frac{5}{6} - \frac{1}{2\lambda}]^4 \\
\mathcal{S}_{B_5 B_5} &= [\frac{5}{3} - \frac{2}{\lambda}]^2[\frac{2}{3}]^5[\frac{3}{\lambda} - 1][\frac{3}{\lambda} - \frac{2}{3}][\frac{1}{\lambda}]^5[\frac{1}{3} + \frac{1}{\lambda}]^3[\frac{4}{3} - \frac{2}{\lambda}]^3[\frac{2}{\lambda}][\frac{4}{3} - \frac{1}{\lambda}]^2
\end{aligned}$$

$$\begin{aligned}
\mathcal{S}_{B_5 K_1} &= \left[\frac{1}{2} - \frac{1}{2\lambda}\right]^2 \left[\frac{5}{6} - \frac{1}{2\lambda}\right]^2 \left[\frac{1}{6} + \frac{3}{2\lambda}\right] \left[\frac{3}{2\lambda} - \frac{1}{6}\right] \\
\mathcal{S}_{B_5 K_2} &= \left[\frac{5}{6}\right]^2 \left[\frac{1}{2}\right]^2 \left[\frac{7}{6} - \frac{1}{\lambda}\right]^2 \left[\frac{5}{6} - \frac{1}{\lambda}\right]^3 \left[\frac{1}{2} + \frac{1}{\lambda}\right] \left[\frac{2}{\lambda} - \frac{1}{6}\right] \left[\frac{2}{\lambda} - \frac{1}{2}\right]
\end{aligned} \tag{4.8}$$

The complete mass spectrum is given in appendix A, and the full set of fusings for generic values of  $q$  is summarised in appendix B. Appendix D contains a detailed description of the pole structures of all S-matrix amplitudes appearing for  $\lambda \leq \frac{9}{4}$ . Closed scattering diagrams, such as the ones shown earlier, have been constructed for all poles not associated with bound states in this region. In figure 13 we show one particularly-elusive example.

### 4.3 Problems for $\lambda > 9/4$

For  $\lambda > 9/4$ , we have not been able to close the bootstrap. The only exception is the point  $\lambda = 5/2$ , for which  $q = 1$ , the kink states decouple, and the breather sector reproduces the minimal  $E_8$  S-matrix. Away from this point, our difficulties may simply be due to a failure to spot the necessary Coleman-Thun diagrams; on the other hand, they may hint at a genuine breakdown of the bootstrap programme. In the following we shall mention some of the problems that we encountered, in the hope of contributing to further work on these issues.

Many of the poles in the already-described S-matrix elements can be explained all the way up to  $\lambda = 3$ . However, the Coleman-Thun diagrams for some poles do not close for  $\lambda > 9/4$ , a sign that new particles may need to be introduced. Consider first the poles in  $S_{B_3 B_3}$  at  $\frac{1}{\lambda}$ , in  $S_{B_2 B_2}$  at  $\frac{1}{\lambda} - \frac{1}{3}$ , and in  $S_{B_2 B_5}$  at  $\frac{1}{3} + \frac{1}{2\lambda}$ . Once  $\lambda$  passes  $9/4$ , the residues of these poles do not change sign, and if all are provisionally associated with forward-channel bound states, the masses of these states as calculated from the formula

$$m_c^2 = m_a^2 + m_b^2 - 2m_a m_b \cos(\pi u_{ab}^c) \tag{4.9}$$

(where  $u_{ab}^c$  is the fusing angle  $t$  at which the pole occurs) all coincide. It is therefore natural to assign these poles to a single new breather state  $B_6$ . From (4.9), its mass is  $4m \cos(\frac{\pi}{2} - \frac{\pi}{\lambda}) \cos(\frac{\pi}{6} - \frac{\pi}{2\lambda})$ . The other fusing angles for this putative particle follow from (4.9) on permuting the labels  $a, b$  and  $c$ , and all turn out to have simple (constant plus linear) dependencies on  $\frac{1}{\lambda}$ ; they are listed explicitly in appendix C.

A similar story can be told for the poles in  $S_{B_1 B_5}$  and  $S_{B_3 B_3}$  at  $\frac{2}{\lambda} - \frac{2}{3}$ , leading us to introduce a further breather  $B_7$  with mass  $8m \cos(\frac{\pi}{2} - \frac{\pi}{2\lambda}) \cos(\frac{\pi}{6} - \frac{\pi}{2\lambda}) \cos(\frac{\pi}{3} - \frac{\pi}{\lambda})$ . However, the (fifth-order) pole in  $S_{B_5 B_5}$  at  $\frac{1}{\lambda}$ , which corresponds to  $B_8$  at  $\lambda = 5/2$ , is more enigmatic. First, we note that it overlaps with an odd-order pole at  $\lambda = 12/5$ , causing its residue to change sign. This might suggest that the identification of the direct and cross channel poles should be swapped at this point, though since the pole is of higher order it is not possible to say definitively that this must happen (cf. the discussions in [21]). As mentioned in appendix D, bound state poles in some kink scattering amplitudes also have crossovers, but for these the S-matrix contrives to preserve the signs of the residues. It is also worth noticing that some of the S-matrix elements involving  $B_8$  have physical-strip zeroes for  $\lambda < 12/5$ . There is no a-priori

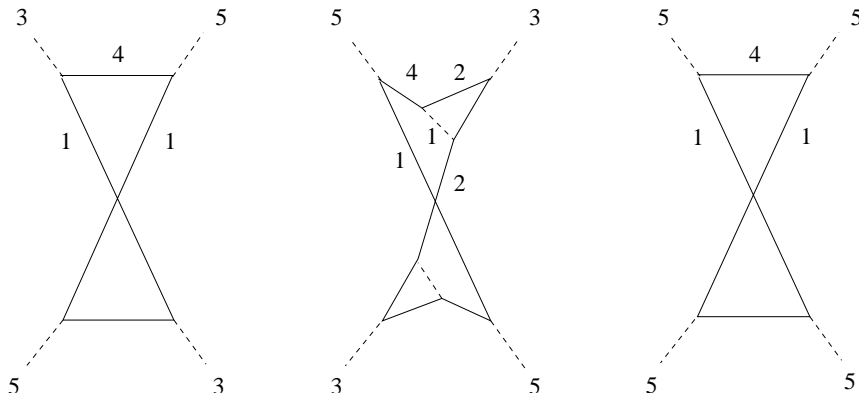


Figure 14: Closed scattering diagrams without corresponding poles in the S-matrix

reason why this should not occur, but it breaks the pattern seen for all other S-matrix elements up to this value of  $\lambda$ . These two problems together make our identification of the  $B_8$  particle somewhat tentative for  $\lambda \leq 12/5$ .

The worries about the  $B_8$  particle would probably be resolved if other, more serious, difficulties could be overcome. A number of poles remain unexplained for  $\lambda > 9/4$  even after the introduction of  $B_6$ ,  $B_7$  and  $B_8$ . Many have residues which change sign, suggesting that for at least some range of  $\lambda$  they will not correspond to bound states. Of those which don't, the poles at  $\frac{2}{3} - \frac{3}{2\lambda}$  in  $S_{K_1K_2}$ ,  $\frac{1}{6}$  in  $S_{B_2K_1}$ ,  $\frac{1}{\lambda}$  in  $S_{B_3K_1}$ ,  $\frac{1}{6} + \frac{3}{2\lambda}$  in  $S_{B_5K_1}$ ,  $\frac{1}{\lambda} - \frac{1}{6}$  in  $S_{B_1K_2}$ , and  $\frac{1}{3} + \frac{1}{2\lambda}$  in  $S_{B_3K_2}$  give rise to kinks of the same mass. Calling this particle  $K_4$ , we could similarly identify another kink  $K'_4$  with the poles at  $\frac{3}{2\lambda} - \frac{1}{6}$  in  $S_{B_5K_1}$  and in  $\frac{3}{2\lambda} - \frac{1}{3}$  in  $S_{B_3K_2}$ . However, the introduction of these new particles is problematic for a number of reasons. Most fundamentally, and in contrast to the situation for  $B_6$ ,  $B_7$  and  $B_8$ , some fusing angles involving  $K_4$  and  $K'_4$ , calculated using (4.9), are *not* simple functions of  $\frac{1}{\lambda}$ . As a result, the inclusion of  $K_4$  or  $K'_4$  in closed scattering diagrams for already-introduced particles predicts poles which do not appear in their S-matrix elements. For example, the diagrams shown in figure 14 can be drawn if  $K_4$  is included in the spectrum. In addition, the irrationality of the fusing angles leads to a breakdown of the conserved charge bootstrap, forcing higher-spin charges to be zero. This makes it highly unlikely that  $K_4$  and  $K'_4$  should be added to the spectrum of the model.

On the other hand, we have not been able to account for the would-be  $K_4$  and  $K'_4$  poles in the manner of Coleman and Thun, using the set of particles and fusings that we have already identified. Take the  $\frac{2}{3} - \frac{3}{2\lambda}$  pole in  $S_{K_1K_2}$  as an example. This pole is simple, so if the Coleman-Thun mechanism is to be invoked, the naive order of poles from the relevant on-shell diagrams must be reduced in some way. One tactic is to search for closed scattering diagrams involving only kinks as internal states, in order to get cancellations in sums over S-matrix elements of the sort seen in earlier sections.

Such diagrams must have the form shown in figure 15.

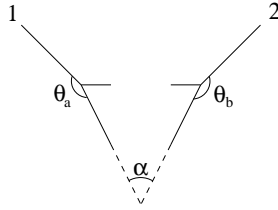


Figure 15: Difficulties in finding Coleman-Thun diagrams for  $S_{K_1 K_2}$

A quick check of the options for  $\theta_a$  and  $\theta_b$  shows that the scattering angle between the outermost internal lines  $\alpha = -\frac{4}{3} - \frac{3}{2\lambda} + \theta_a + \theta_b$  is always less than zero, and so no closed diagram can be constructed. Similar arguments hold for other poles, in particular those in the  $S_{B_3 K_1}$  and  $S_{B_5 K_1}$  amplitudes that were mentioned above.

In the absence of a satisfactory explanation for these poles, the closure of the bootstrap is still an open question. There remains one further possibility: new particles might enter the spectrum which are not simple bound states of any of the already-existing particles, so that their masses would not be immediately visible in the existing S-matrix elements. This would mimic the situation which would arise in the sine-Gordon model if one only knew of the breather particles, and wanted to deduce the presence of the solitons by looking at breather scattering alone. It is very hard to rule this out, but further work will be needed before we can tell whether it offers a way to escape from the problems discussed in this section.

#### 4.4 Other work on $\phi_{12}$ perturbations

Since our results on  $\phi_{12}$  perturbations are incomplete, it is particularly important to compare them with other work. We begin by mentioning the points  $\lambda = 2, \frac{9}{4}$  and  $\frac{5}{2}$ , which correspond to the minimal  $E_6, E_7$  and  $E_8$  S-matrices. These are rather special, as for these values of  $\lambda$ ,  $q$  is an integer. Not only do various poles overlap, but also some instances of the Coleman-Thun mechanism break down. This is because the total contribution associated with a given on-shell diagram can involve factors of  $q - (\text{integer})$  (equations (3.7), (3.11) and (3.12) provide some examples of this phenomenon). This means that, exceptionally, these poles do *not* have Coleman-Thun explanations when  $q$  hits integer values, and this requires the introduction of ‘exceptional’ bound states in order to complete the bootstrap at these points. The  $K_3$  kink state at the  $E_7$  point, and the  $B_4$  breather at the  $E_8$  point, appear to have this evanescent status. In addition, the overlapping of the poles allows a number of extra couplings to appear, and this should be borne in mind before worrying that the tables of couplings in appendices B and C seems small in comparison with tables for Toda models given in [22]. These subtleties aside, the S-matrices at the exceptional points are perfectly self-consistent. Their physical-strip pole structures match those of affine Toda field theories, and the extensive discussions contained in [22, 21] can be borrowed to verify that all higher poles can be described via the Coleman-Thun mechanism.

Away from integer values of  $q$ , some general aspects of the spectrum of  $\phi_{12}$ -perturbed minimal models were discussed by Smirnov in [2], while the particular case of  $\mathcal{M}_{56} + \phi_{12}$  was treated by Martins in [23] and by Koubek in [24]. In none of these papers was a complete analysis of pole structures attempted, but other aspects permit comparisons to be made. In the papers of Smirnov and Koubek,  $\lambda$  corresponds to  $\frac{\pi}{\xi}$ , and  $\theta \rightarrow \beta$ .

In [2], Smirnov gave an initial description of the spectrum implied by his S-matrix, concentrating mainly on points related to perturbations of unitary minimal models. The chief difference between Smirnov's S-matrix and that of Chim and Zamolodchikov is a matter of kink structure, so one would expect the two to agree on the spectrum of bound states and the diagonal scattering amplitudes. Indeed, while explicit formulae for the remaining S-matrix elements were not given in [2], Smirnov comments that the spectrum for  $\phi_{12}$  perturbations settles down to four particles for (his)  $\xi \geq \pi/2$ . In our notation this is  $\lambda \leq 2$ , and so this regime of  $\phi_{12}$  perturbations corresponds to the range  $3/2 < \lambda \leq 2$  discussed in §4.1, for which we did indeed find four particles. Furthermore, the masses are easily checked to agree, and so all is consistent.

Referring to (2.32), the  $\phi_{12}$  perturbation of  $\mathcal{M}_{56}$  discussed in [23] and [24], should correspond to  $\lambda = \frac{21}{10}$ , which lies in the region where we predicted six particles. In [23], Martins made a detailed numerical study of the finite-volume spectrum of  $\mathcal{M}_{56} + \phi_{12}$  using the truncated conformal space approach. (He also discussed some subtleties relating to the choice of modular invariant for the unperturbed theory; as mentioned above, we do not expect this to affect the full spectrum of particle masses when the theories are considered on the infinite line.) High-mass states were hard to detect, but he was able to predict the presence of five particles, which in our notation are  $K_1$ ,  $B_1$ ,  $K_2$ ,  $B_2$  and  $B_3$ , with numerically-obtained values for the masses which are consistent with predictions from the exact S-matrix. The remaining particle,  $B_5$ , has a much higher mass and so its absence from the numerical data of [23] is no surprise.

This case was further examined in [24]. Translating from our notation to that of [24],  $[a] \leftrightarrow \langle a \rangle$ ,  $B_2^{(\text{ref. [24]})} = B_3^{(\text{us})}$  and  $B_4^{(\text{ref. [24]})} = B_5^{(\text{us})}$ . However, the mass of the breather identified in [24] as  $B_3^{(\text{ref. [24]})}$  is also equal to that of  $B_3^{(\text{us})}$ , which is already in the spectrum at  $\lambda < 2$ . As can be seen from appendix A, the other extra breather to enter the spectrum for  $\lambda > 2$ ,  $B_2^{(\text{us})}$ , has a mass less than that of  $B_3^{(\text{us})}$ , which perhaps explains why it was missed in [24]. As a result of this problem, the spectrum and S-matrix given in [24] are unfortunately incomplete, but insofar as they go and modulo some further typos, they are otherwise consistent with our results, specialised to  $\lambda = \frac{21}{10}$ .

Finally, we should mention that S-matrices for  $\phi_{12}$  perturbations of minimal models  $\mathcal{M}_{2,2n+1}$  were discussed in [25]. These theories have  $\lambda = 3n$  in our notation, and hence are a long way from the region  $\lambda \in [\frac{3}{2}, 3]$  relevant to tricritical scaling Potts models – in particular, the perturbing operator always has a negative scaling dimension apart from the somewhat-trivial case of  $n=1$ . Perhaps more to the point, they also all correspond formally to  $q = 0$ , and the simplifications of the scattering theory at such points [2] make it hard to draw any general lessons. Nevertheless, it is interesting that the bootstrap can be closed at least at some locations beyond the region that we were able to treat.



## 5 Conclusions

In this paper we have given what to the best of our knowledge is the first complete treatment of the pole structure and bootstrap for the critical and tricritical Potts models. For all of the critical models, and for the tricritical models with  $4 > q > 2$ , we have found a spectrum of particles such that *all* S-matrix poles have potential field-theoretical explanations. This has been achieved by a novel variant of the Coleman-Thun mechanism, taking into account the formal counting of intermediate vacua at general values of  $q$ . The cancellations are at times extremely intricate, and we take this success as offering retrospective justification of our approach, though a rigorous framework is still lacking.

Our calculations have proceeded on a case-by case (or rather, pole-by-pole) basis, which becomes increasingly laborious as the number of particles increases. It is tempting to suppose that there must be a better way to do all of this, if only the relevant underlying structure could be identified. For the much-simpler examples of the ADE-related diagonal scattering theories, a universal understanding of bootstrap closure has been achieved using a construction of the S-matrix elements based on the theory of root systems [26,27], and it would be very interesting to have a similar treatment for general  $q$ -state Potts models. At present this seems to be a long way off, though the results of Oota [28], extending the root systems approach to cover the non simply-laced Toda theories, may be a sign that things are not completely hopeless. (Further discussions of the hidden geometry of affine Toda field theory can be found in [29,30,16,31].)

The most important outstanding question left by our work concerns the situation for  $\lambda > \frac{9}{4}$ , where we were unable to complete the bootstrap. Problems with bootstrap closure have been encountered a couple of times before. In [32], the intricacy of the mass spectrum for general complex  $a_2^{(1)}$  Toda theory is discussed. In Smirnov's approach, the Potts S-matrices are associated with  $a_2^{(2)}$ ; given the relations between  $a_2^{(1)}$  and  $a_2^{(2)}$  it is reasonable to hope that our results even for  $\lambda < \frac{9}{4}$  may be of some relevance to these issues. However, since the situation for  $a_2^{(1)}$  is likely to be at least as complicated as that for  $a_2^{(2)}$ , this may not be the best place to look for hints as to how to close the bootstrap for  $\lambda > \frac{9}{4}$ . Rather, it seems more promising to investigate further perturbations of minimal models, for which there are at least techniques such as the TCSA to fall back on. In situations where the Potts ground state (generated by the identity operator) and the minimal model ground state (generally generated by some negative-dimension operator) become degenerate in infinite volume, we would expect scaling Potts and perturbed minimal model results to be directly related. Difficulties with the bootstrap for the models  $\mathcal{M}_{3,5}$  and  $\mathcal{M}_{3,7}$  perturbed by  $\phi_{12}$  have been remarked by Mussardo and Takacs [33], though as these theories have  $\lambda = \frac{7}{2}$  and  $\frac{11}{2}$ , they are not directly relevant to our current concerns. The interval  $\frac{9}{4} < \lambda < 3$  corresponds, via (2.32), to  $\frac{5}{4} < \frac{p'}{p} < \frac{3}{2}$ , and any information on  $\phi_{12}$  perturbations of these minimal models, away from the  $E_8$  point  $\frac{p'}{p} = \frac{4}{3}$ , would be extremely interesting, as would any indications of extra pathologies in such cases.

We end with a curious piece of numerology. Recall that as the parameter  $\lambda$  runs from

0 to 3, we pass first through the critical and then the tricritical scaling Potts models. At rational values of  $\lambda$ , the theories are also associated with  $\phi_{21}$  or  $\phi_{12}$  perturbations of minimal models. But some points are even more special, in that their minimal models can be realised as ‘diagonal’ coset conformal field theories of the form  $g^{(1)} \times g^{(1)}/g^{(2)}$ , with field labelled by  $(1, 1, \text{ad})$  always being the perturbing operator. (See, for example, chapter 18 of [34] and references therein for more on the coset construction.) These points, together with the corresponding values of  $q$  and  $c$ , are listed in appendix A, and they suggest that the scaling Potts models provide a structure which unifies the following sequence of Lie algebras:

$$\{ A_1, A_2, G_2, D_4, F_4, E_6, E_7, E_8 \} \quad (5.1)$$

Remarkably, the same sequence has appeared in the pure mathematics literature, in the work of Vogel, Deligne, Cohen and de Man, Cvitanovic and others – see [35, 36, 38, 37, 39, 41, 40] for a selection of references. This set of algebras, sometimes referred to as ‘the’ exceptional series, is picked out by a number of special properties – for example, the tensor products  $\text{ad} \otimes \text{ad}$  decompose in a uniform way (Deligne proposed that this should extend to higher powers  $\otimes^k \text{ad}$ , and conjectured that this could be explained by the existence of some more general class of objects, depending on a parameter  $t$ , which specialise to the representations of the members of the exceptional series at certain values of  $t$ ). The algebras also make up the extended last line of the Freudenthal magic square (in this context, it is interesting that an appearance of the magic square has been noted, on a case-by-case basis, in studies of  $R$ - and  $K$ - matrices and the Yang-Baxter equation (see for example [42])). However, the deep sense in which the algebras (5.1) form a family is still rather mysterious, and so the fact that they are found in connection with the *continuous* set of Potts models seems to be quite suggestive. Inspired by this coincidence, we can consider an alternative labelling of the Potts models, by setting

$$h^\vee(\lambda) = \frac{6\lambda}{3-\lambda} . \quad (5.2)$$

This parameter coincides with the dual Coxeter number of the relevant algebra at the special points, where it is also related to the parameter  $a$  used in [36, 37] by  $h^\vee = 1/a$ . Two more interesting properties can now be noted - first, the ‘natural’ range for  $\lambda$ ,  $[0, 3]$ , is mapped to the range  $[0, \infty]$  for  $h^\vee$ . At the Lie algebra related points,  $h^\vee$  is in some senses a measure of the complexity of the corresponding scattering theory, so this suggests that  $\lambda = 3$  may indeed be some sort of natural boundary also from the S-matrix point of view. Second, there is one more special point for the Potts models, labelled ‘P’ in appendix A and corresponding to  $\lambda = \frac{1}{2}$ , which is  $q = 1$  on the critical branch – the percolation point. It is natural to add this point to our list, as it then gives the special points a symmetry under  $\lambda \rightarrow 3-\lambda$ . One might worry that this would spoil the nice match with the exceptional series of Lie algebras, but in [36], Deligne remarks that it is natural to add the trivial group  $e$  to the list (5.1), so long as it is assigned the dual Coxeter number  $6/5$ . This is precisely the value that the Potts models would suggest, if the percolation value  $\lambda = \frac{1}{2}$  is substituted into (5.2).

In fact, the exceptional series has (at least) one further member: in [38], Deligne and de Man remark that the superalgebra  $OSp(1|2)$ , with dual Coxeter number  $3/2$ , can be added between  $e$  and  $A_1$ . (This to some degree explains the fact, already noted by Cohen and de Man in [37], that for  $h^\vee = 3/2$  various dimension formulae take integer values.) Can we find a rôle for this superalgebra in the Potts story? The answer turns out to be yes. Inverting (5.2),  $h^\vee = 3/2$  corresponds to  $\lambda = 3/5$ ,  $q = (5 - \sqrt{5})/2$  and  $c = 8/35$ . The construction of diagonal coset models based on Lie superalgebras seems to be relatively unexplored territory, but some facts about the relevant affine superalgebras are known. In particular, the level  $k$   $OSp(1|2)$  central charge is

$$c(OSp(1|2)^{(k)}) = \frac{2k}{2k+3} \quad (5.3)$$

(see, for example, [43] and references therein). Assuming that no subtleties interfere with the usual calculation, we then expect

$$c\left(\frac{OSp(1|2)^{(1)} \times OSp(1|2)^{(1)}}{OSp(1|2)^{(2)}}\right) = \frac{8}{35} \quad (5.4)$$

which is exactly the required value. Note that this is the central charge of a non-unitary minimal model,  $\mathcal{M}_{7,10}$ . This does not contradict its being realised as a coset, since superalgebras are involved. While not all fields of the nonunitary model appear in the corresponding Potts model, the identity and the energy operator are present, and at least in this sense we can claim to have found the superalgebra  $OSp(1|2)$  to be embedded into the continuous family of  $q$ -state Potts models.

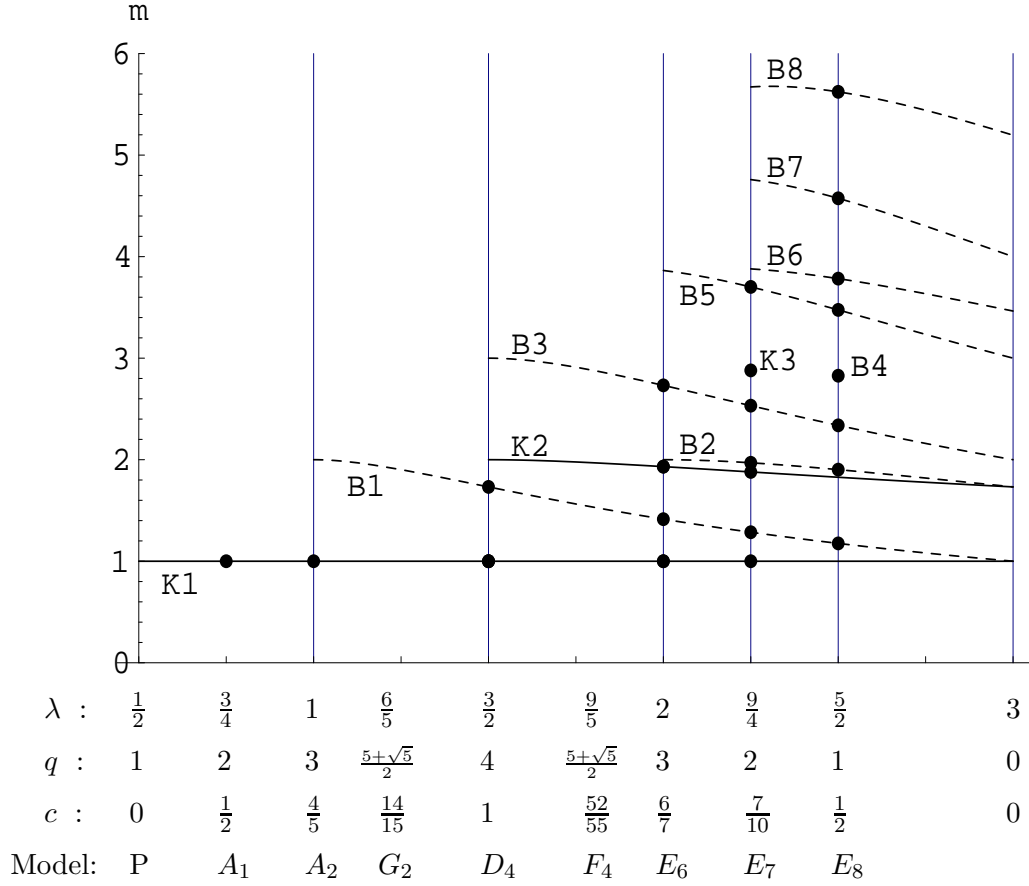
Cohen and de Man [37] found one further point at which integers appear in dimension formulae: translating into our notations it is  $h^\vee = 24$ ,  $\lambda = 12/5$ . As far as we are aware, no group-theoretical interpretation of this point is known, but from the Potts perspective it should be related to the tricritical model at  $q = (5 - \sqrt{5})/2$ , or the  $\phi_{12}$  perturbation of the minimal model  $\mathcal{M}_{10,13}$  (with central charge  $38/65$ ). This is particularly tantalising: lying between the  $E_7$  and  $E_8$  points,  $\lambda = 12/5$  is in the region where we have not been able to close the bootstrap, and any new information might give us the necessary hint to resolve the problems described in §4.3 above. Furthermore, there are independent reasons to think that  $\lambda = 12/5$  might be special: as mentioned in §4.3, for  $\lambda > 12/5$  the S-matrix elements involving  $B_8$  have no physical-strip zeroes, perhaps signalling that this is the point at which the  $B_8$  particle enters the spectrum.

While we do not have any explanation as yet for why the link between the Potts models and the exceptional sequence of Lie (super-)algebras should be so neat, we feel that the coincidences are sufficiently striking to merit further investigation. A better understanding might shed light both on the structure of the Potts model S-matrices, and on the deeper meaning of the exceptional series and the Deligne conjecture.

**Acknowledgements** — This paper has been a long time in the writing, during the course of which we have benefitted from discussions and correspondence with John

Cardy, Aldo Delfino, Clare Dunning, Davide Fioravanti, Philippe di Francesco, Paul Fendley, Alan Macfarlane, Barry McCoy, Giuseppe Mussardo, Bill Oxbury, Marco Picco, Hubert Saleur, Tony Sudbery, Gabor Takacs, Ole Warnaar, Gerard Watts and Jean-Bernard Zuber. In addition, PED thanks the YITP, Kyoto, for hospitality. Visits of PED to YITP were funded by a Daiwa-Adrian Prize and a Royal Society / JSPS Anglo-Japanese Collaboration grant, title 'Symmetries and integrability'. RT thanks the EPSRC for an Advanced Fellowship, and AJP thanks the JSPS and the FAPESP for postdoctoral fellowships.

## A The mass spectrum



$$m_{K_1} = m$$

$$m_{B_1} = 2m \cos\left(\frac{\pi}{2} - \frac{\pi}{2\lambda}\right)$$

$$m_{K_2} = 2m \cos\left(\frac{\pi}{3} - \frac{\pi}{2\lambda}\right)$$

$$m_{B_3} = 4m \cos\left(\frac{\pi}{2} - \frac{\pi}{2\lambda}\right) \cos\left(\frac{\pi}{2\lambda} - \frac{\pi}{6}\right)$$

$$m_{B_2} = 2m \cos\left(\frac{\pi}{2} - \frac{\pi}{\lambda}\right)$$

$$m_{B_5} = 4m \cos\left(\frac{\pi}{2} - \frac{\pi}{\lambda}\right) \cos\left(\frac{\pi}{3} - \frac{\pi}{2\lambda}\right)$$

$$m_{B_6} = 4m \cos\left(\frac{\pi}{2} - \frac{\pi}{\lambda}\right) \cos\left(\frac{\pi}{6} - \frac{\pi}{2\lambda}\right)$$

$$m_{B_7} = 8m \cos\left(\frac{\pi}{2} - \frac{\pi}{2\lambda}\right) \cos\left(\frac{\pi}{6} - \frac{\pi}{2\lambda}\right) \cos\left(\frac{\pi}{3} - \frac{\pi}{\lambda}\right)$$

$$m_{B_8} = 8m \cos\left(\frac{\pi}{2} - \frac{\pi}{\lambda}\right) \cos\left(\frac{\pi}{3} - \frac{\pi}{2\lambda}\right) \cos\left(\frac{\pi}{2\lambda}\right).$$

The breather states are labelled so as to be mass-ordered at the  $E_8$  point  $\lambda = \frac{5}{2}$ ; note also that the states  $K_3$  and  $B_4$  are only present in the model for  $\lambda = \frac{9}{4}$  and

$\frac{5}{2}$  respectively, for reasons that were explained in §4.4. The solid dots indicate the mass spectra of the diagonal scattering theories which occur at integer values of  $q$ . For  $\lambda > \frac{9}{4}$ , the mass spectrum is almost certainly incomplete, save for the  $E_8$  point  $\lambda = \frac{5}{2}$ ; in addition, as discussed in §4.3, it is possible that the appearance of the  $B_8$  particle should be postponed to  $\lambda > \frac{12}{5}$ . In the list of model identifications, ‘P’ indicates that the theory at  $\lambda = \frac{1}{2}$  is related to the percolation problem. The remaining entries are Lie algebras  $g$ , and signal that the corresponding model is related to a perturbation of the  $g^{(1)} \times g^{(1)}/g^{(2)}$  coset conformal field theory by its  $(1, 1, \text{adj})$  operator.

## B Fusings and fusing angles for $\lambda < 9/4$

This table summarises the fusings and fusing angles between particles in the region where we have been able to close the bootstrap. Each entry shows the particles which can be found as bound states of the particles listed along the top and left of the table, together with the angle  $t$  at which each fusing occurs. Depending on the value of  $\lambda$ , some of the bound states may be absent from the spectrum. In such cases, the corresponding pole is either off the physical strip, or else has a Coleman-Thun explanation.

	$K_1$	$B_1$	$K_2$	$B_3$	$B_2$	$B_5$	
$K_1$	$K_1 \quad \frac{2}{3}$ $B_1 \quad 1 - \frac{1}{\lambda}$ $K_2 \quad \frac{2}{3} - \frac{1}{\lambda}$ $B_2 \quad 1 - \frac{2}{\lambda}$	$K_1 \quad \frac{1}{2} + \frac{1}{2\lambda}$ $K_2 \quad \frac{1}{6} + \frac{1}{2\lambda}$	$K_1 \quad \frac{2}{3} + \frac{1}{2\lambda}$ $B_1 \quad 1 - \frac{1}{2\lambda}$ $B_3 \quad 1 - \frac{3}{2\lambda}$	$K_2 \quad \frac{1}{\lambda} + \frac{1}{3}$	$K_1 \quad \frac{1}{2} + \frac{1}{\lambda}$		
$B_1$		$B_1 \quad \frac{2}{3}$ $B_3 \quad \frac{1}{\lambda} - \frac{1}{3}$ $B_2 \quad \frac{1}{\lambda}$	$K_1 \quad \frac{5}{6}$	$B_1 \quad \frac{7}{6} - \frac{1}{2\lambda}$ $B_2 \quad \frac{1}{2} + \frac{1}{2\lambda}$ $B_5 \quad \frac{3}{2\lambda} - \frac{1}{2}$	$B_1 \quad 1 - \frac{1}{2\lambda}$ $B_3 \quad \frac{2}{3} - \frac{1}{2\lambda}$	$B_3 \quad \frac{4}{3} - \frac{1}{\lambda}$	
$K_2$			$K_2 \quad \frac{2}{3}$ $B_5 \quad 1 - \frac{2}{\lambda}$	$K_1 \quad \frac{2}{3} + \frac{1}{2\lambda}$		$K_2 \quad \frac{1}{2} + \frac{1}{\lambda}$	
$B_3$				$B_3 \quad \frac{2}{3}$	$B_1 \quad \frac{5}{6}$	$B_1 \quad \frac{7}{6} - \frac{1}{2\lambda}$	
$B_2$					$B_2 \quad \frac{2}{3}$ $B_5 \quad \frac{2}{3} - \frac{1}{\lambda}$	$B_2 \quad \frac{2}{3} + \frac{1}{2\lambda}$	
$B_5$						$B_5 \quad \frac{2}{3}$	

As mentioned in §4.4, exceptional couplings appear at the points  $\lambda = 2, \frac{9}{4}, \frac{5}{2}$ . Rather than tabulate them here, we refer the reader to [22] for complete listings.

## C Extra fusings and fusing angles for $\lambda > 9/4$

Our results are incomplete for  $\lambda > 9/4$ , and we cannot be sure that the bootstrap closes at all. However, there is good evidence for the existence of at least three further particles, namely  $B_6$ ,  $B_7$  and  $B_8$ . The first two we expect to be present for all  $\lambda > 9/4$ , while  $B_8$  may only enter the spectrum for  $\lambda > 12/5$ . The following table summarises the additional fusings and fusing angles involving these new particles. Further particles cannot be ruled out (indeed, they are most probably required if the bootstrap is to close) and so we do not claim that this list is exhaustive.

	$B_3$	$B_2$	$B_5$	$B_6$	$B_7$	$B_8$
$B_1$			$B_7 \quad \frac{2}{\lambda} - \frac{2}{3}$		$B_5 \quad \frac{3}{2} - \frac{3}{2\lambda}$	
$B_3$	$B_6 \quad \frac{1}{\lambda}$ $B_7 \quad \frac{2}{\lambda} - \frac{2}{3}$			$B_3 \quad 1 - \frac{1}{2\lambda}$	$B_3 \quad \frac{4}{3} - \frac{1}{\lambda}$	
$B_2$		$B_6 \quad \frac{1}{\lambda} - \frac{1}{3}$	$B_6 \quad \frac{1}{3} + \frac{1}{2\lambda}$	$B_2 \quad \frac{7}{6} - \frac{1}{2\lambda}$ $B_5 \quad \frac{5}{6} - \frac{1}{2\lambda}$ $B_8 \quad \frac{3}{2\lambda} - \frac{1}{2}$		$B_6 \quad \frac{4}{3} - \frac{1}{\lambda}$
$B_5$			$B_8 \quad \frac{1}{\lambda}$	$B_2 \quad \frac{5}{6}$	$B_1 \quad \frac{7}{6} - \frac{1}{2\lambda}$	$B_5 \quad 1 - \frac{1}{2\lambda}$
$B_6$				$B_6 \quad \frac{2}{3}$		$B_2 \quad \frac{7}{6} - \frac{1}{2\lambda}$
$B_7$					$B_7 \quad \frac{2}{3}$	
$B_8$						$B_8 \quad \frac{2}{3}$

## D Bound state poles of the S-matrix for $\lambda < 9/4$

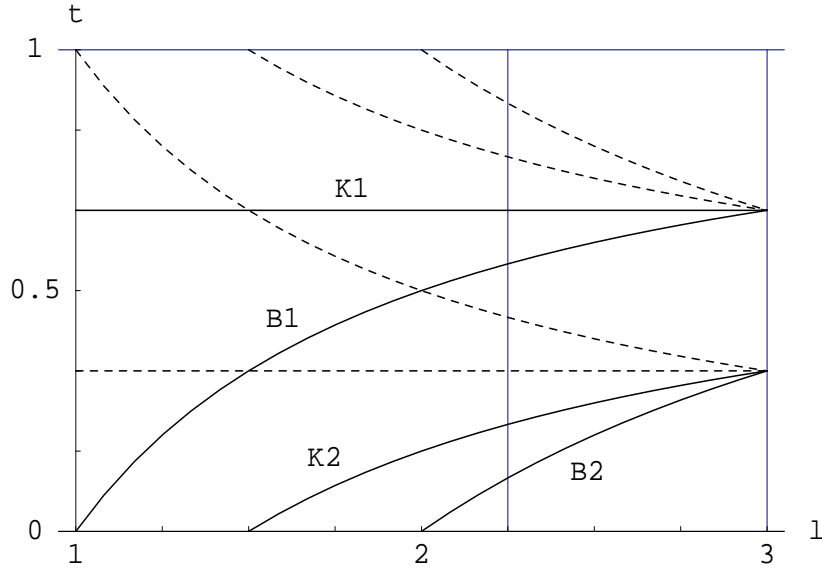
In this appendix we summarise the bound states of the scattering amplitudes which appear for  $\lambda \leq \frac{9}{4}$ . For the kink-kink amplitudes, the physical strip pole contents of each separate amplitude are given in tables 3, 5 and 6 of the main text; here we show their locations (though not their orders) with a symbol  $[x]$ , indicating that the combined set of amplitudes has poles at  $t = x$  and at  $t = 1 - x$ . The poles of the other S-matrix elements can be read off quite easily from their explicit formulae – in the following, we add a subscript  $a$  to a block  $[x]$  to signify that  $a$  appears as forward-channel bound state of that scattering process, at  $\theta = i\pi x$ . A question mark indicates that, at least for some range of  $\lambda \in (\frac{9}{4}, 3]$ , the corresponding pole is currently unexplained. In spite of the problems in completing the bootstrap in the interval  $\frac{9}{4} < \lambda < \frac{5}{2}$ , at  $\lambda = \frac{5}{2}$  (ie.

$q = 1$ ) the S-matrix is well behaved and reduces to that of the  $E_8$  related model.

In the plots,  $t = \frac{\theta}{i\pi}$  as in the main text, and  $l = \lambda$ . Double lines denote poles of even order. Grey shading denotes presence of a higher order scattering process for that pole. In general, direct channel poles have solid lines and cross channel poles have dashed lines - for poles with no associated bound states the choice is arbitrary. Forward-channel bound state poles are identified on the graphs by the relevant particle, while dotted grey shading indicates poles for which we have yet to find a satisfactory explanation. The crossings-over of poles in the  $K_1 K_1$  and  $K_1 K_2$  scattering amplitudes cause no problems for the assignment of forward and crossed channels, as the amplitudes affected -  $\mathcal{S}_1$  and  $\mathcal{S}_2$  at  $\lambda = \frac{3}{2}$ , and  $\mathcal{S}_3$  at  $\lambda = 2$  - vanish at these points. This extra zero in the non-scalar factors changes the analytic continuation, preserving the signs of the residues.

In each graph, the value  $\lambda = \frac{9}{4}$  is indicated by a vertical line. Beyond this point the problems mentioned in §4.3 set in, and our results must be considered to be incomplete.

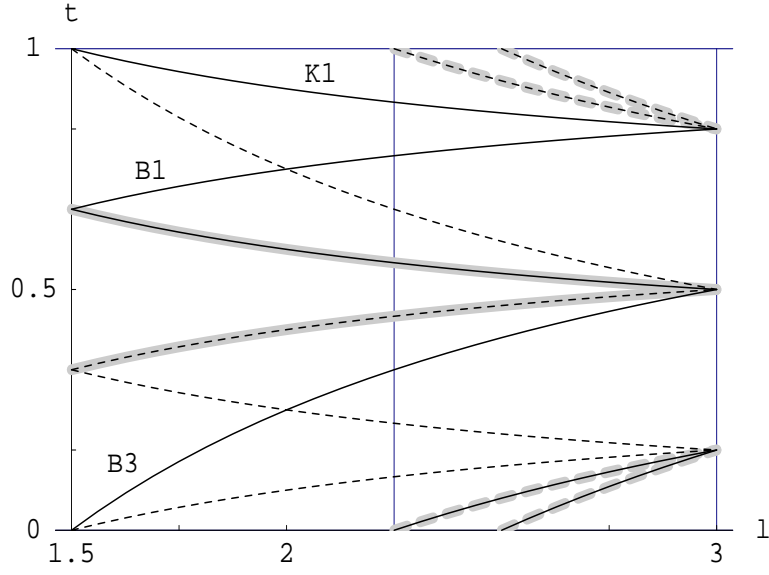
### D.1 Kink-kink S-matrix elements



Bound state poles of  $\mathcal{S}_{K_1 K_1}^0$ ,  $\mathcal{S}_{K_1 K_1}^1$ ,  $\mathcal{S}_{K_1 K_1}^2$  and  $\mathcal{S}_{K_1 K_1}^3$

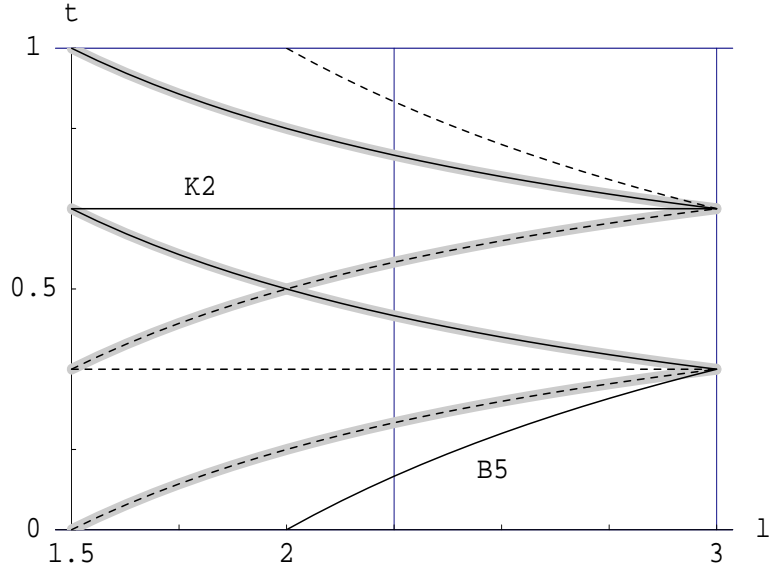
Pole locations:  $[\frac{2}{3}]_{K_1}$   $[\frac{2}{3} - \frac{1}{\lambda}]_{K_2}$   $[1 - \frac{1}{\lambda}]_{B_1}$   $[1 - \frac{2}{\lambda}]_{B_2}$





Bound state poles of  $\mathcal{S}_{K_2K_1}^0$ ,  $\mathcal{S}_{K_2K_1}^1$ ,  $\mathcal{S}_{K_2K_1}^2$  and  $\mathcal{S}_{K_2K_1}^3$

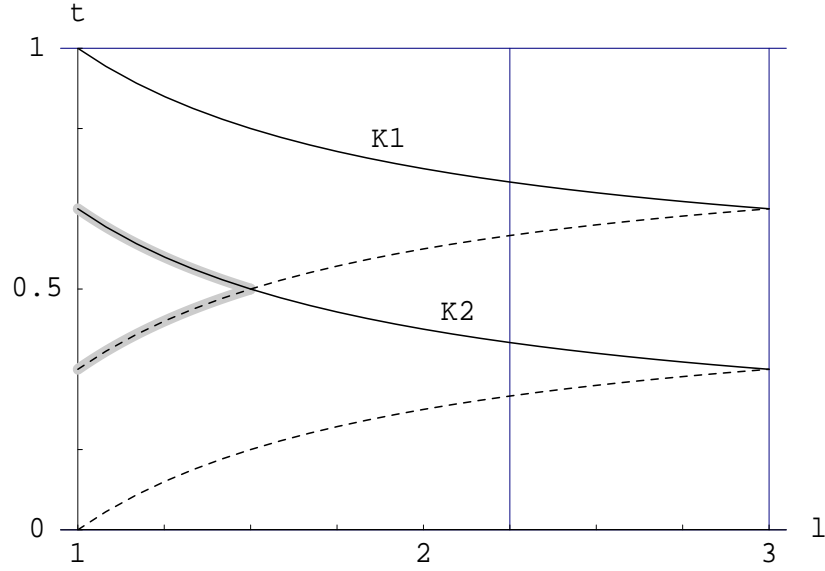
Pole locations:  $[\frac{2}{3} + \frac{1}{2\lambda}]_{K_1} [1 - \frac{1}{2\lambda}]_{B_1} [1 - \frac{3}{2\lambda}]_{B_3} [\frac{1}{3} + \frac{1}{2\lambda}] [\frac{2}{3} - \frac{3}{2\lambda}]_? [1 - \frac{5}{2\lambda}]_?$



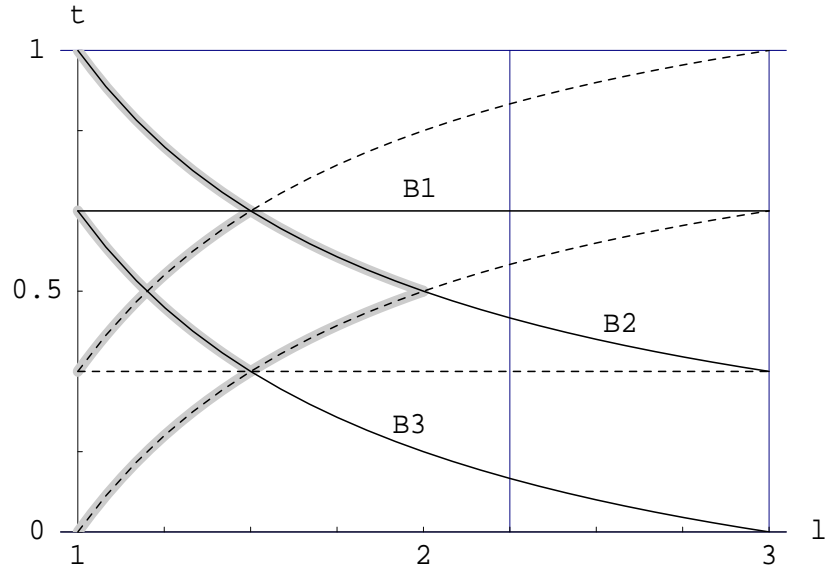
Bound state poles of  $\mathcal{S}_{K_2K_2}^0$ ,  $\mathcal{S}_{K_2K_2}^1$ ,  $\mathcal{S}_{K_2K_2}^2$  and  $\mathcal{S}_{K_2K_2}^3$

Pole locations:  $[\frac{2}{3}]_{K_2} [1 - \frac{2}{\lambda}]_{B_5} [\frac{2}{3} - \frac{1}{\lambda}] [1 - \frac{1}{\lambda}]$

**D.2 Kink-breather and breather-breather S-matrix elements,**  
 $1 < \lambda \leq \frac{3}{2}$

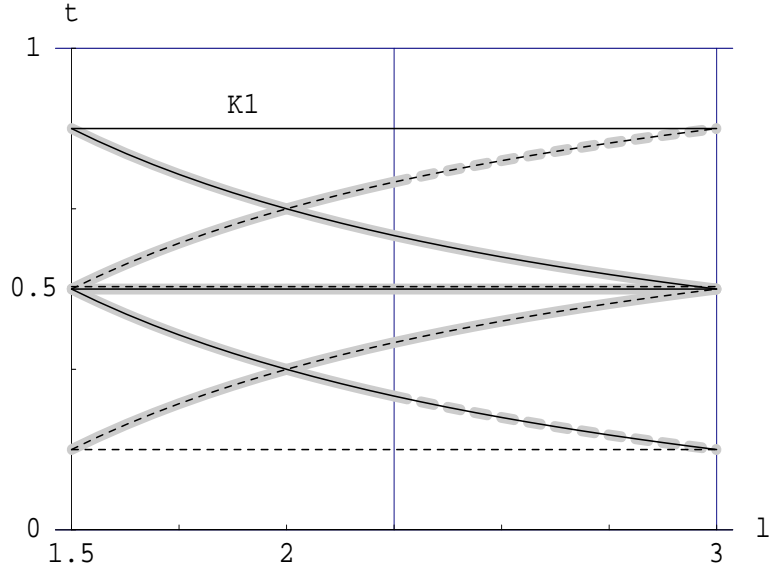


$$\mathcal{S}_{B_1 K_1} = \left[\frac{1}{2} + \frac{1}{2\lambda}\right]_{K_1} \left[\frac{1}{6} + \frac{1}{2\lambda}\right]_{K_2}$$

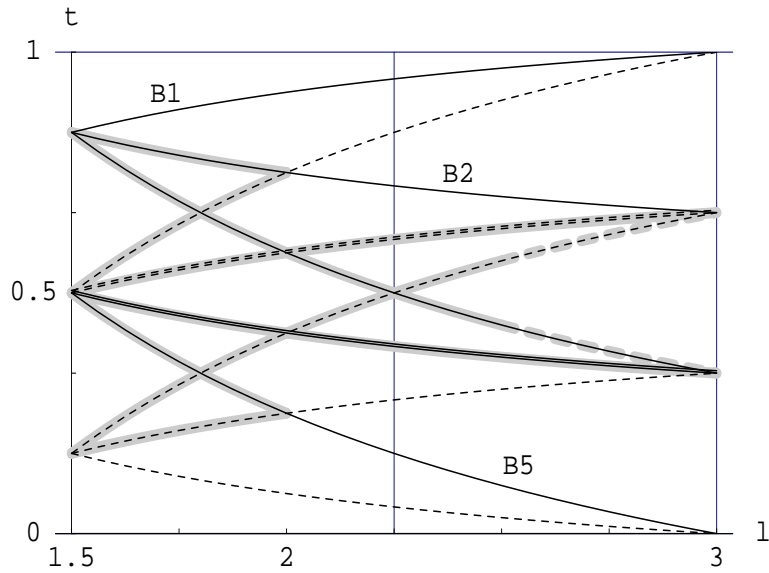


$$\mathcal{S}_{B_1 B_1} = \left[\frac{2}{3}\right]_{B_1} \left[\frac{1}{\lambda}\right]_{B_2} \left[\frac{1}{\lambda} - \frac{1}{3}\right]_{B_3}$$

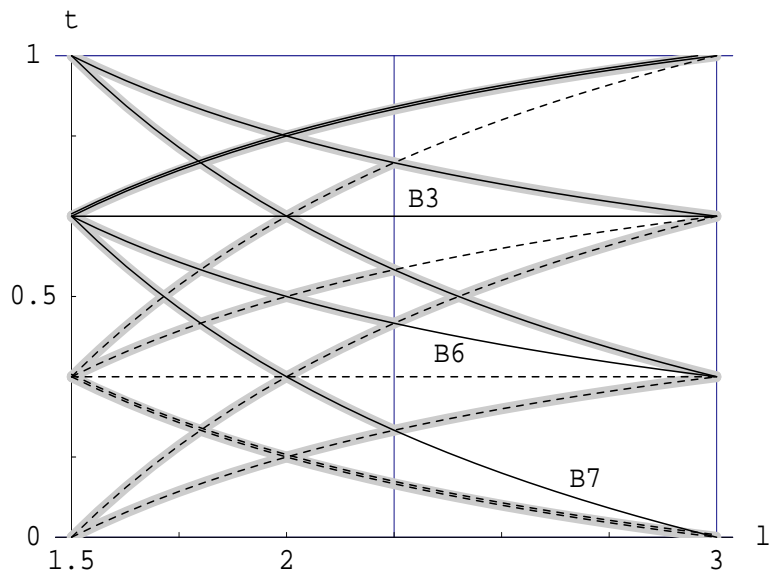
**D.3 Additional kink-breather and breather-breather S-matrix elements for  $\frac{3}{2} < \lambda \leq 2$**



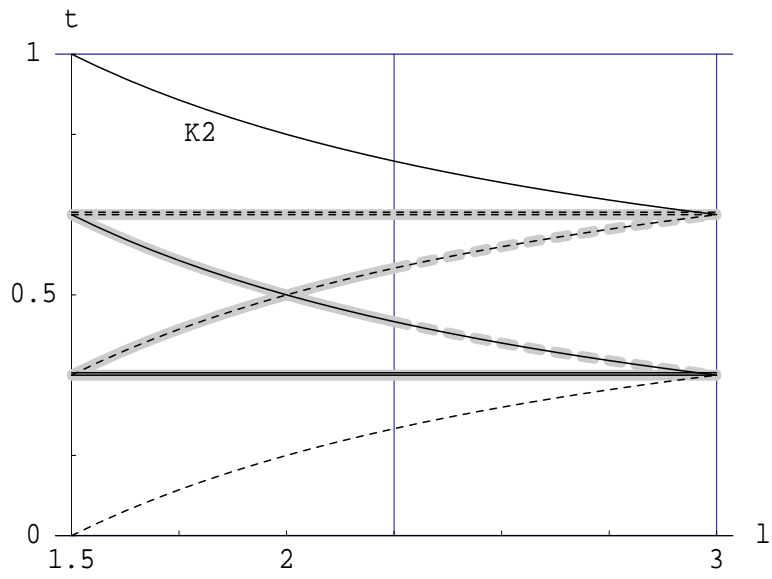
$$\mathcal{S}_{B_1 K_2} = [\frac{1}{2}][\frac{5}{6}]_{K_1} [\frac{1}{6} + \frac{1}{\lambda}][\frac{1}{\lambda} - \frac{1}{6}]?$$



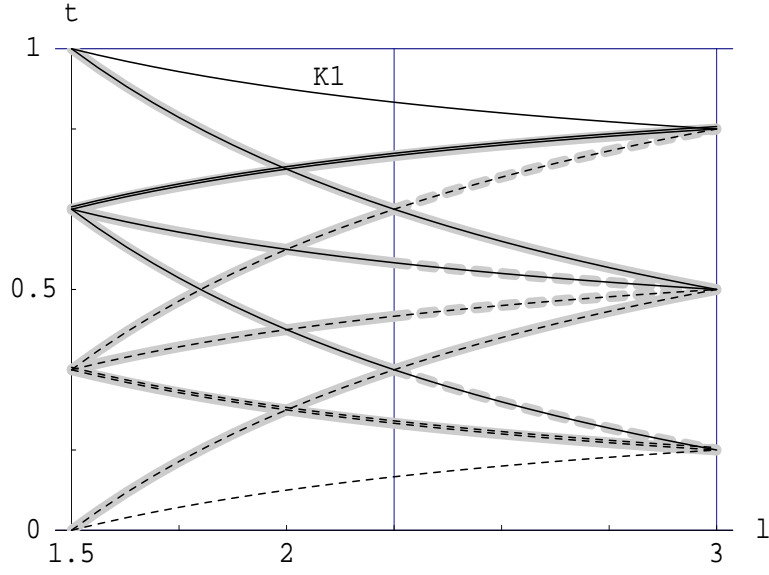
$$\mathcal{S}_{B_1 B_3} = [\frac{1}{6} + \frac{1}{2\lambda}]^2 [\frac{1}{2} + \frac{1}{2\lambda}]_{B_2} [\frac{7}{6} - \frac{1}{2\lambda}]_{B_1} [\frac{3}{2\lambda} - \frac{1}{2}]_{B_5} [\frac{3}{2\lambda} - \frac{1}{6}]?$$



$$\mathcal{S}_{B_3 B_3} = \left[ \frac{2}{3} \right]_{B_3}^3 \left[ \frac{1}{\lambda} \right]_{B_6}^3 \left[ \frac{4}{3} - \frac{1}{\lambda} \right]^2 \left[ \frac{1}{3} + \frac{1}{\lambda} \right] \left[ \frac{2}{\lambda} - \frac{2}{3} \right]_{B_7} \left[ \frac{2}{\lambda} - \frac{1}{3} \right]$$

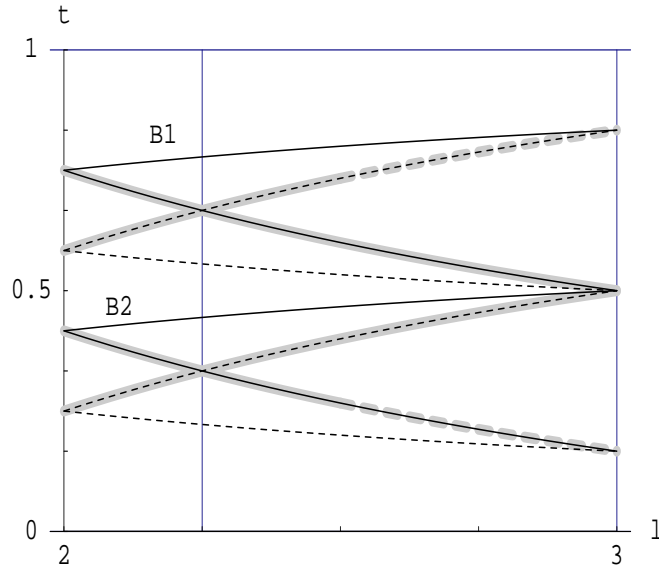


$$\mathcal{S}_{B_3 K_1} = \left[ \frac{1}{3} \right]^2 \left[ \frac{1}{\lambda} \right]_{K_2} \left[ \frac{1}{\lambda} + \frac{1}{3} \right]$$

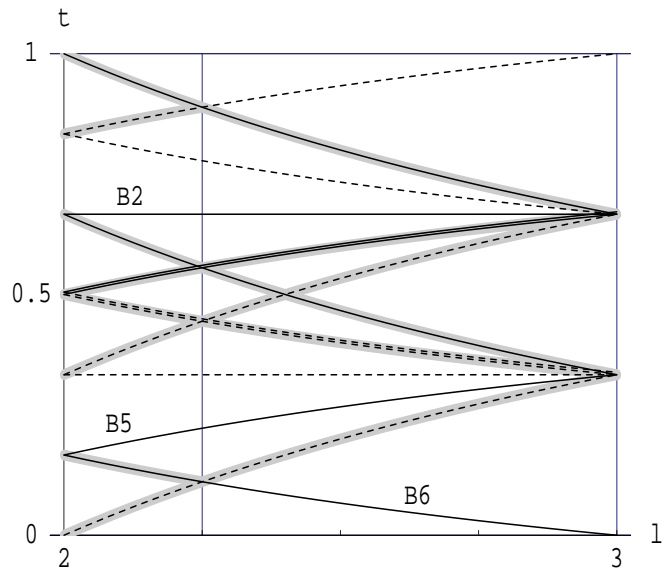


$$\mathcal{S}_{B_3 K_2} = [1 - \frac{1}{2\lambda}]^2 [\frac{1}{3} + \frac{1}{2\lambda}]^3 [\frac{2}{3} + \frac{1}{2\lambda}] K_1 [\frac{3}{2\lambda} - \frac{1}{3}] [\frac{3}{2\lambda}]$$

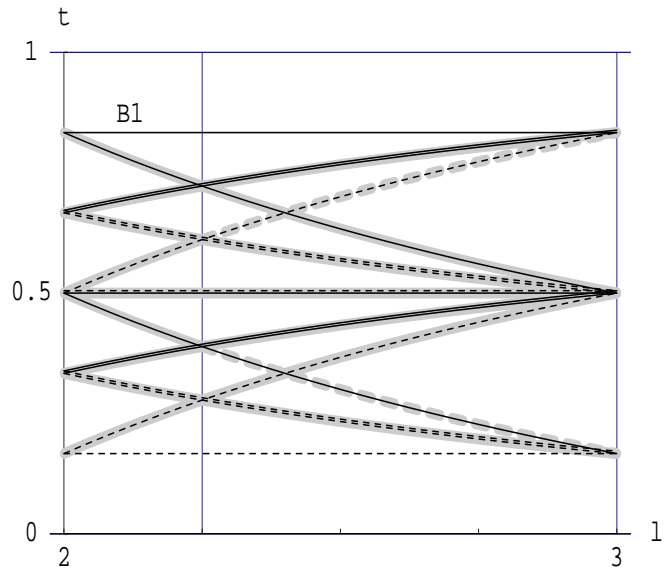
#### D.4 Additional kink-breather and breather-breather S-matrix elements for $2 < \lambda \leq \frac{9}{4}$



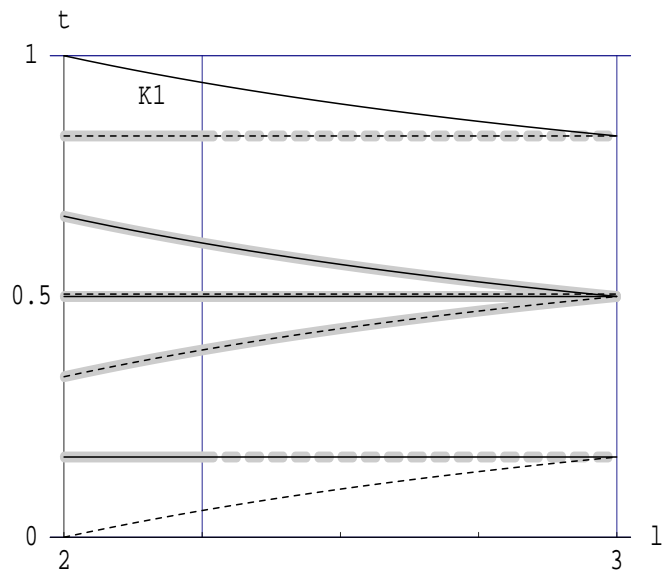
$$\mathcal{S}_{B_1 B_2} = [1 - \frac{1}{2\lambda}]_{B_1} [\frac{2}{3} - \frac{1}{2\lambda}]_{B_3} [\frac{3}{2\lambda}] [\frac{3}{2\lambda} - \frac{1}{3}]$$



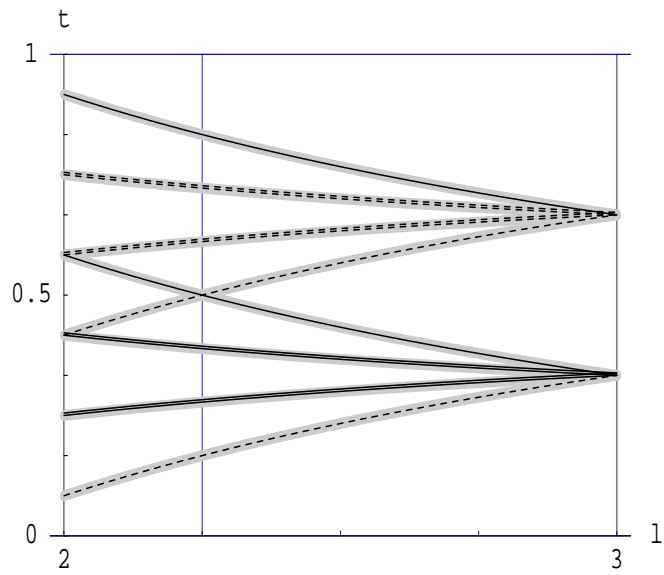
$$\mathcal{S}_{B_2 B_2} = \left[\frac{2}{3}\right]_{B_2} \left[\frac{2}{3} - \frac{1}{\lambda}\right]_{B_5} \left[\frac{1}{\lambda} - \frac{1}{3}\right]_{B_6} \left[\frac{2}{\lambda}\right] \left[\frac{2}{\lambda} - \frac{1}{3}\right] \left[1 - \frac{1}{\lambda}\right]^2$$



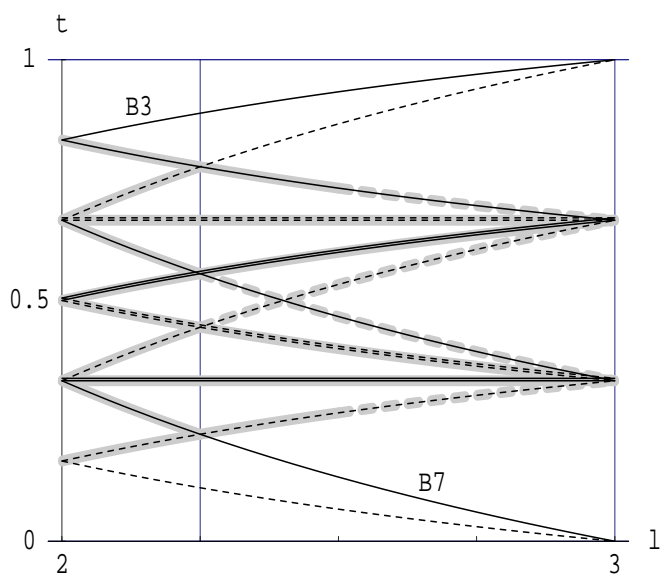
$$\mathcal{S}_{B_2 B_3} = \left[\frac{1}{2}\right] \left[\frac{5}{6}\right]_{B_1} \left[\frac{2}{\lambda} - \frac{1}{6}\right] \left[\frac{7}{6} - \frac{1}{\lambda}\right]^2 \left[\frac{2}{\lambda} - \frac{1}{2}\right] \left[\frac{5}{6} - \frac{1}{\lambda}\right]^2$$



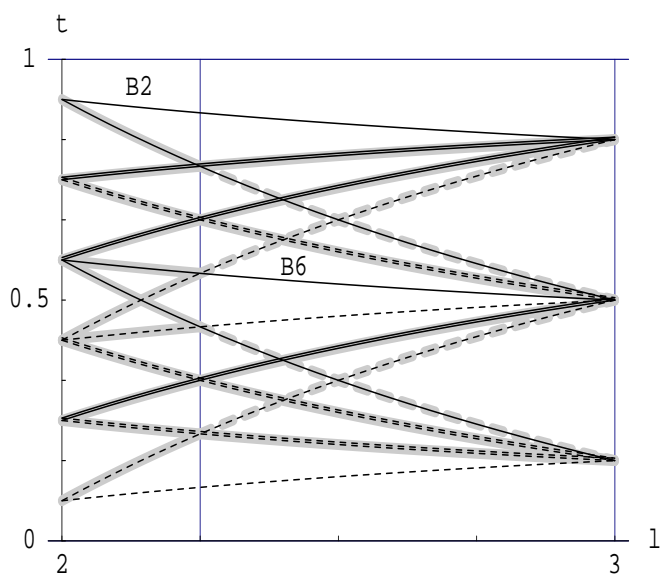
$$\mathcal{S}_{B_2 K_1} = \left[\frac{1}{2}\right]\left[\frac{1}{6}\right] \left[\frac{1}{2} + \frac{1}{\lambda}\right]_{K_1} \left[\frac{1}{6} + \frac{1}{\lambda}\right]$$



$$\mathcal{S}_{B_2 K_2} = \left[\frac{1}{2} - \frac{1}{2\lambda}\right]^2 \left[\frac{1}{6} + \frac{1}{2\lambda}\right]^2 \left[\frac{1}{6} + \frac{3}{2\lambda}\right] \left[\frac{3}{2\lambda} - \frac{1}{6}\right]$$

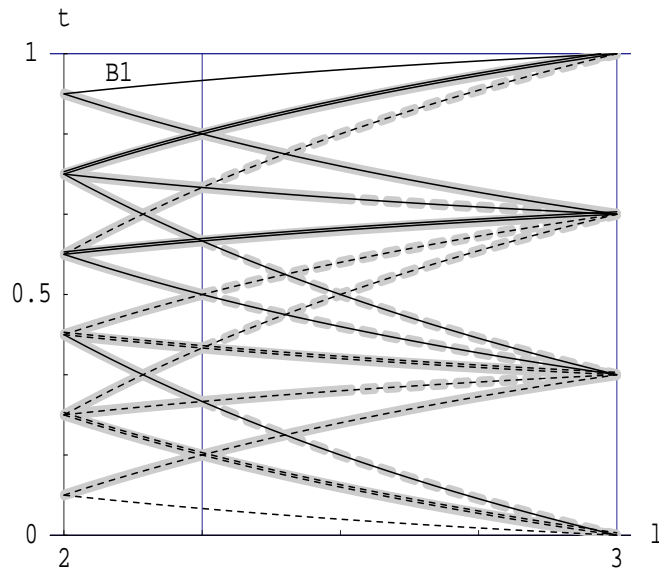


$$\mathcal{S}_{B_1 B_5} = \left[\frac{1}{3}\right]^2 \left[\frac{4}{3} - \frac{1}{\lambda}\right]_{B_3} \left[\frac{1}{3} + \frac{1}{\lambda}\right]_? \left[\frac{2}{\lambda} - \frac{2}{3}\right]_{B_7} \left[\frac{2}{\lambda} - \frac{1}{3}\right]_? \left[1 - \frac{1}{\lambda}\right]^2$$

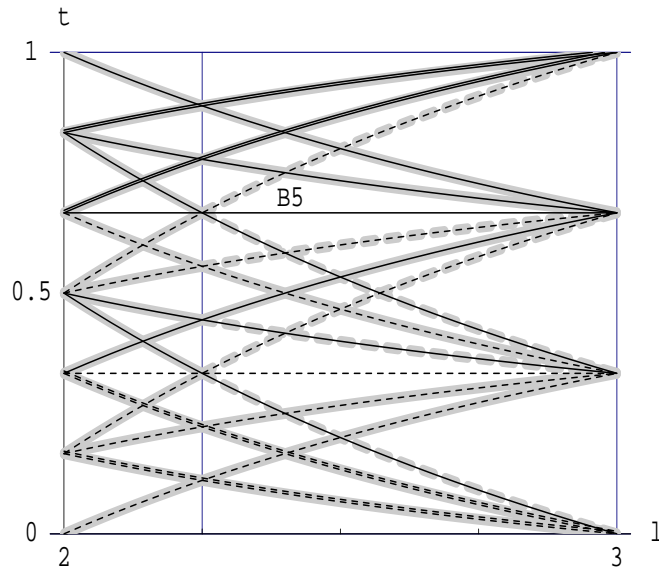


$$\mathcal{S}_{B_2 B_5} = \left[\frac{4}{3} - \frac{3}{2\lambda}\right]^2 \left[1 - \frac{3}{2\lambda}\right]^2 \left[\frac{2}{3} + \frac{1}{2\lambda}\right]_{B_2} \left[\frac{1}{3} + \frac{1}{2\lambda}\right]_{B_6}^3 \left[1 - \frac{1}{2\lambda}\right]^2 \left[\frac{5}{2\lambda} - \frac{1}{3}\right]_? \left[\frac{5}{2\lambda} - \frac{2}{3}\right]_?$$

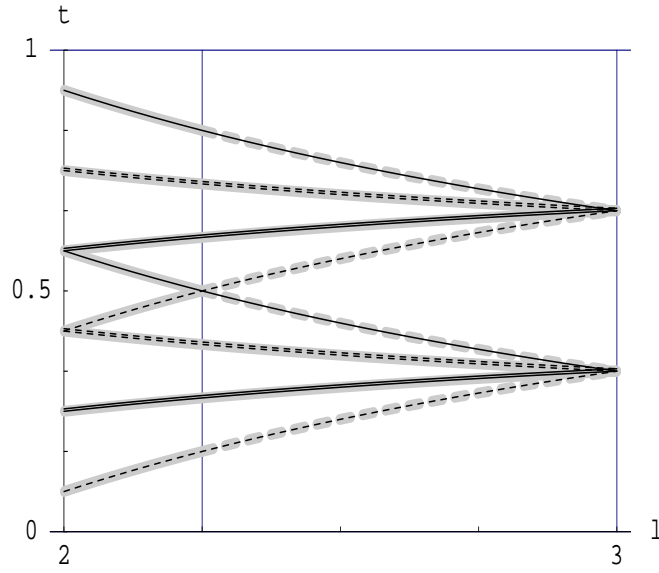




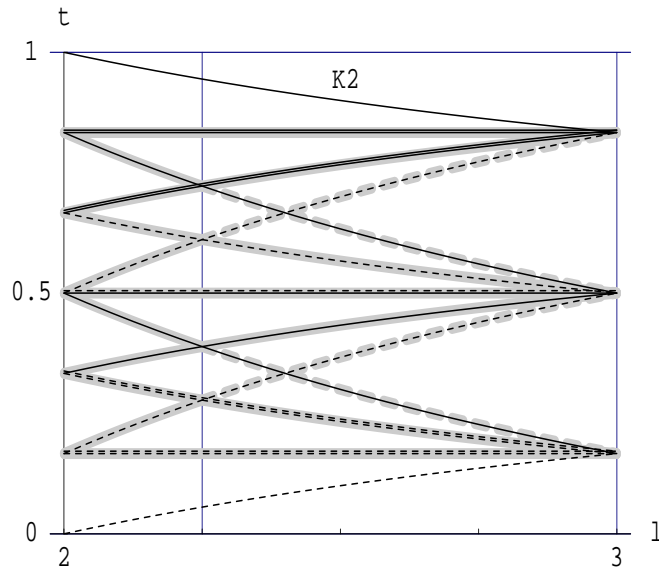
$$\mathcal{S}_{B_3 B_5} = \left[\frac{7}{6} - \frac{1}{2\lambda}\right]_{B_1} \left[\frac{1}{6} + \frac{3}{2\lambda}\right] \left[\frac{3}{2} - \frac{3}{2\lambda}\right]^2 \left[\frac{5}{2\lambda} - \frac{5}{6}\right] \left[\frac{1}{2} + \frac{1}{2\lambda}\right]^3 \left[\frac{3}{2\lambda} - \frac{1}{6}\right]^3 \left[\frac{5}{2\lambda} - \frac{1}{2}\right] \left[\frac{5}{6} - \frac{1}{2\lambda}\right]^4$$



$$\mathcal{S}_{B_5 B_5} = \left[\frac{5}{3} - \frac{2}{\lambda}\right]^2 \left[\frac{2}{3}\right]_{B_5}^5 \left[\frac{3}{\lambda} - 1\right] \left[\frac{3}{\lambda} - \frac{2}{3}\right] \left[\frac{1}{\lambda}\right]^5 \left[\frac{1}{3} + \frac{1}{\lambda}\right]^3 \left[\frac{4}{3} - \frac{2}{\lambda}\right]^3 \left[\frac{2}{\lambda}\right] \left[\frac{4}{3} - \frac{1}{\lambda}\right]^2$$



$$\mathcal{S}_{B_5K_1} = \left[\frac{1}{2} - \frac{1}{2\lambda}\right]^2 \left[\frac{5}{6} - \frac{1}{2\lambda}\right]^2 \left[\frac{1}{6} + \frac{3}{2\lambda}\right] \left[\frac{3}{2\lambda} - \frac{1}{6}\right]$$



$$\mathcal{S}_{B_5K_2} = \left[\frac{5}{6}\right]^2 \left[\frac{1}{2}\right]^2 \left[\frac{7}{6} - \frac{1}{\lambda}\right]^2 \left[\frac{5}{6} - \frac{1}{\lambda}\right]^3 \left[\frac{1}{2} + \frac{1}{\lambda}\right]_{K_2} \left[\frac{2}{\lambda} - \frac{1}{6}\right] \left[\frac{2}{\lambda} - \frac{1}{2}\right]$$

## References

- [1] L. Chim and A.B. Zamolodchikov, ‘Integrable field theory of q-state Potts model with  $0 < q < 4$ ’, Int. J. Mod. Phys. A7 (1992) 5317–5335
- [2] F.A. Smirnov, ‘Exact S-matrices for  $\phi_{12}$ -Perturbated minimal models of conformal field theory’, Int. J. Mod. Phys. A6 (1991) 1407–1428

- [3] E.M. Fortuin and P. Kasteleyn, ‘On the random-cluster model.1. Introduction and relation to other models.’, *Physica* 57, (1972) 536–564
- [4] P. Fendley and N. Read, ‘Exact S-matrices for supersymmetric sigma models and the Potts model’, [hep-th/0207176](#)
- [5] P. Dorey, A. Pocklington and R. Tateo, ‘Integrable aspects of the scaling q-state Potts models II: finite-size effects’, preprint DCPT-02/53
- [6] V.S. Dotsenko, ‘Critical behaviour and associated conformal algebra of the  $\mathbb{Z}_3$  Potts model’, *Nucl. Phys. B*235 (1984) 54–74
- [7] B. Nienhuis, A.N. Berker, E.K. Riedel and M. Schick, ‘First- and second-order phase transitions in Potts models: renormalization-group solution’, *Phys. Rev. Lett.* 43 (1979) 737
- [8] T.W. Burkhardt, ‘Critical and tricritical exponents of the Potts lattice gas’, *Z. Phys. B* (1980) 159
- [9] B. Nienhuis, ‘Analytical calculation of two leading exponents of the dilute Potts model’, *J. Phys. A*15 (1982) 199–213
- [10] P. di Francesco, H. Saleur and J.-B. Zuber, ‘Relations between the Coulomb Gas Picture and Conformal Invariance of Two-Dimensional Critical Models’ *J. Stat. Phys.* 49 (1987), 57–79
- [11] A.B. Zamolodchikov, ‘Integrable Field Theory from Conformal Field Theory’, *Proceedings of Taniguchi Symposium, Kyoto* (1988)
- [12] G. Delfino and J.L. Cardy, ‘Universal amplitude ratios in the two-dimensional q-state Potts model and percolation from quantum field theory’, *Nucl. Phys. B*519 (1998) 551, [hep-th/9712111](#)
- [13] V.S. Dotsenko and V.A. Fateev, ‘Conformal algebra and multipoint correlation functions in two-dimensional statistical models’, *Nucl. Phys. B*240 (1984) 312
- [14] S. Parke, ‘Absence Of Particle Production And Factorization Of The S Matrix In (1+1)-Dimensional Models’, *Nucl. Phys. B*174 (1980) 166.
- [15] S. Coleman and H.J. Thun, ‘On the prosaic origin of the double poles in the sine-Gordon S-matrix’, *Commun. Math. Phys.* 61 (1978) 31
- [16] P. Dorey, ‘Exact S-matrices’, *Proceedings of the 1996 Eötvös Graduate School* (Springer 1997) 85–125, [hep-th/9810026](#)
- [17] E. Corrigan, P.E. Dorey and R. Sasaki, ‘On a generalised bootstrap principle’, *Nucl. Phys. B*408 (1993) 579, [hep-th/9304065](#)
- [18] P. Dorey, R. Tateo and G.M.T. Watts, ‘Generalisations of the Coleman-Thun mechanism and boundary reflection factors’, *Phys. Lett. B*448 (1999) 249, [hep-th/9810098](#)

- [19] H.W. Braden, E. Corrigan, P.E. Dorey and R. Sasaki, ‘Extended Toda field theory and exact S-matrices’, *Phys. Lett.* B227 (1989) 411
- [20] A. Pocklington, ‘Bulk and boundary scattering in the q-state Potts model’, Ph.D thesis, Durham, 1998
- [21] H.W. Braden, E. Corrigan, P.E. Dorey and R. Sasaki, ‘Multiple poles and other features of affine Toda field theory’ *Nucl. Phys.* B356 (1991) 469–498
- [22] H.W. Braden, E. Corrigan, P.E. Dorey and R. Sasaki, ‘Affine Toda field theory and exact S-matrices’, *Nucl. Phys.* B338 (1990) 689–746
- [23] M. J. Martins, ‘The off critical behavior of the multicritical Ising models’, *Int. J. Mod. Phys.* A7 (1992) 7753
- [24] A. Koubek, ‘S matrices of  $\phi_{1,2}$ -perturbed minimal models: IRF formulation and bootstrap program’, *Int. J. Mod. Phys.* A9 (1994) 1909
- [25] A. Koubek, M. J. Martins and G. Mussardo, ‘Scattering matrices for  $\phi_{1,2}$  perturbed conformal minimal models in absence of kink states’, *Nucl. Phys.* B368 (1992) 591
- [26] P. Dorey, ‘Root systems and purely elastic S matrices’, *Nucl. Phys.* B358 (1991) 654–676
- [27] P. Dorey, ‘Root systems and purely elastic S matrices II’, *Nucl. Phys.* B374 (1992) 741–761, [hep-th/9110058](#)
- [28] T. Oota, ‘q deformed Coxeter element in nonsimply laced affine Toda field theories’, *Nucl. Phys.* B504 (1997) 738–752, [hep-th/9706054](#)
- [29] A. Fring and D.I. Olive, ‘The Fusing rule and the scattering matrix of affine Toda theory’, *Nucl. Phys.* B379 (1992) 429–447
- [30] P. Dorey, ‘Hidden geometrical structures in integrable models’, in the proceedings of the NATO ARW *Integrable quantum field theories*, Como (Plenum 1993), [hep-th/9212143](#)
- [31] A. Fring, C. Korff and B.J. Schulz, ‘On the universal representation of the scattering matrix of affine Toda field theory’, *Nucl. Phys.* B567 (2000) 409–453, [hep-th/9907125](#)
- [32] H. Saleur and B. Wehefritz-Kaufmann, ‘Thermodynamics of the complex SU(3) Toda theory’, *Phys. Lett.* B481 (2000), 419–426, [hep-th/0003217](#)
- [33] G. Mussardo and G. Takacs, unpublished
- [34] P. Di Francesco, P. Mathieu and D. Senechal, *Conformal Field Theory*, New York, USA: Springer (1997)
- [35] P. Vogel, ‘Algebraic structures on modules of diagrams’, *preprint*

- [36] P. Deligne, ‘La série exceptionnelle des groupes de Lie’, C. R. Acad. Sci. Paris 322, Série 1 (1996) 321–326
- [37] A.M. Cohen and R. de Man, ‘Computational evidence for Deligne’s conjecture regarding exceptional groups’, C. R. Acad. Sci. Paris 322, Série 1 (1996) 427–432
- [38] P. Deligne et R. de Man, ‘La série exceptionnelle des groupes de Lie II’, C. R. Acad. Sci. Paris 323, Série 1 (1996) 577–582
- [39] P. Cvitanovic, *Classics illustrated: Group Theory*, Nordita notes (1984); and *Group Theory* webbook at <http://www.nbi.dk/GroupTheory/>
- [40] J.M. Landsberg and L. Manivel, ‘Representation theory and projective geometry’, [math.AG/0203260](https://arxiv.org/abs/math/0203260)
- [41] A.J. Macfarlane and H. Pfeiffer, ‘Representations of the exceptional and other Lie algebras with integral eigenvalues of the Casimir operator’, [math-ph/0208014](https://arxiv.org/abs/math-ph/0208014)
- [42] N.J. MacKay, ‘Rational K-matrices and representations of twisted Yangians’, J. Phys. A35 (2002) 7865–7876, [math.qa/0205155](https://arxiv.org/abs/math/0205155)
- [43] I.P. Ennes, A.V. Ramallo and J.M. Sanchez de Santos, ‘*osp(1|2)* conformal field theory’, in the proceedings of the CERN-Santiago de Compostela-La Plata Meeting *Trends in Theoretical Physics*, La Plata 1997, [hep-th/9708094](https://arxiv.org/abs/hep-th/9708094)